

Alveolar macrophage apoptosis-associated bacterial killing helps prevent murine pneumonia.

Julie A. Preston^{1†}, Martin A. Bewley^{1†}, Helen M. Marriott^{1†}, A. McGarry Houghton², Mohammed Mohasin¹, Jamil Jubrail¹, Lucy Morris¹, Yvonne L. Stephenson¹, Simon Cross¹, David R. Greaves³, Ruth W. Craig⁴, Nico van Rooijen⁵, Colin D. Bingle¹, Robert C. Read⁶, Timothy J. Mitchell⁷, Moira K.B. Whyte⁸, Steven D. Shapiro⁹ and David H. Dockrell^{10*}

¹ The Florey Institute for Host-Pathogen Interactions and Department of Infection, Immunity and Cardiovascular Disease, University of Sheffield Medical School, S10 2RX, UK, ²Division of Pulmonary, Allergy and Critical Care Medicine, University of Pittsburgh Medical Center, USA, ³Sheffield Teaching Hospitals, S10 2RX, UK ³ Sir William Dunn School of Pathology, University of Oxford, OX1 3RF, UK ⁴Department of Pharmacology and Toxicology, Geissel School of Medicine at Dartmouth, 03755, NH, USA, ⁵ Department of Molecular Cell Biology and Immunology, VU University Medical Center, Amsterdam, 1081 HZ, The Netherlands, ⁶University of Southampton Medical School and NIHR Southampton Biomedical Research Centre, Southampton, SO166YD, UK, ⁷ Institute of Microbiology and Infection, School of Immunity and Infection, University of Birmingham, B15 2TT, UK Trust, M23 ⁸Department of Respiratory Medicine and MRC Centre for Inflammation Research, University of Edinburgh. ⁹Division of Pulmonary, Allergy and Critical Care Medicine, University of Pittsburgh Medical Center, USA, ¹⁰ Department of Infection Medicine and MRC Centre for Inflammation Research, University of Edinburgh Corresponding **Author:** David H. Dockrell, The MRC/University of Edinburgh Centre for Inflammation Research, 47 Little France Crescent, Edinburgh, Edinburgh EH16 4TJ UK Phone: +44 (0) 131 242 658 Fax: +44 (0) 131 242 6578 email: david.dockrell@ed.ac.uk.

† These authors contributed equally.

Author contributions: JAP, MAB and HMM contributed equally to this work and generated figures. JAP made and validated the transgenic mouse and performed *in vivo* infections. MAB performed killing assays, flow cytometry, collected data and produced figures. HMM performed *in vivo* experiments involving bone marrow transplantation, neutrophil depletion and designed and conducted experiments involving therapeutic targeting. MH helped design and conduct experiments to generate the transgene construct. DRG designed the CD68 construct. RWC designed the Mcl-1 construct. CDB helped in design of the targeting vector and experiments to evaluate its expression. JJ performed experiments with *S. aureus*. LM performed analysis of BMDM phenotype. YLS and SC performed histopathology. NR provided expertise in liposome experiments. RCR and TJM helped design infection models. JAP, MAB, HMM, MKBW, SS and DHD designed and conceived the experiments. JAP, MAB, HMM, MKW, DRG, RWC, and DHD wrote the manuscript with input from all other authors.

Running Title: Alveolar macrophage apoptosis-associated microbicidal responses

Descriptor Number: 10.9 Pathogen/Host cell interactions

Abstract: 246 Total Word Count 4010

At a glance summary:

1 **Scientific Knowledge on the Subject:** The exact mechanisms used by alveolar
2 macrophages (AM) to kill extracellular bacteria remain unclear.

3 **What This Study Adds to the Field:** We have generated a novel transgenic mouse with
4 AM which over-expresses the anti-apoptotic factor Mcl-1, a molecule that is over-
5 expressed in several patient groups at increased risk of pneumonia, which demonstrates
6 this transgenic has a reduced capacity to clear bacteria from the lung. Apoptosis-
7 associated killing is activated when initial phagolysosomal mechanisms are exhausted
8 and requires a combination of reactive species, including nitric oxide and mitochondrial-
9 derived reactive oxygen species. Re-engaging apoptosis when deficient
10 pharmacologically helps prevent pneumonia in these murine models.

11
12 This article has an online data supplement, which is accessible from this issue's table of
13 content online at www.atsjournals.org

14
15 **Acknowledgements:** This work was funded by a Wellcome Trust Senior Clinical
16 Fellowship (076945) to DHD, by the MRC SHIELD consortium MRNO2995X/1 and by
17 an Innovation grant from the Antimicrobial Resistance Cross Council Initiative supported
18 by the seven research councils (MR/M017931/1) to HMM and MB.

19 The authors thank Jessica Willis and Carl Wright for assisting with murine infection
20 studies.

1 **Abstract**

2
3 **Rationale:** Antimicrobial resistance challenges therapy of pneumonia. Enhancing
4 macrophage microbicidal responses would combat this problem but is limited by our
5 understanding of how alveolar macrophages (AM) kill bacteria.

6 **Objectives:** To define the role and mechanism of AM apoptosis-associated bacterial
7 killing in the lung.

8 **Methods:** We generated a unique CD68.hMcl-1 transgenic mouse with macrophage-
9 specific over-expression of the human anti-apoptotic Mcl-1 protein, a factor upregulated
10 in AM from patients at increased risk of community-acquired pneumonia, to address the
11 requirement for apoptosis-associated killing.

12 **Measurements and Main Results:** Wild-type and transgenic macrophages
13 demonstrated comparable ingestion and initial phagolysosomal killing of bacteria.
14 Continued ingestion (for ≥ 12 h) overwhelmed initial killing and a second late-phase
15 microbicidal response killed viable bacteria in wild-type macrophages, but this response
16 was blunted in CD68.hMcl-1 transgenic macrophages. The late-phase of bacterial killing
17 required both caspase-induced generation of mitochondrial reactive oxygen species
18 (mROS) and nitric oxide (NO), whose peak generation coincided with the late-phase of
19 killing. The CD68.hMcl-1 transgene prevented mROS but not NO generation.

20 Apoptosis-associated killing enhanced pulmonary clearance of *Streptococcus*
21 *pneumoniae* and *Haemophilus influenzae* in wild-type but not CD68.hMcl-1 transgenic
22 mice. Bacterial clearance was enhanced *in vivo* in CD68.hMcl-1 transgenic mice by
23 reconstitution of apoptosis with BH3 mimetics or clodronate-encapsulated liposomes.
24 Apoptosis-associated killing was not activated during *Staphylococcus aureus* lung
25 infection.

26 **Conclusions:** Mcl-1 upregulation prevents macrophage apoptosis-associated killing and
27 establishes that apoptosis-associated killing is required to allow AM to clear ingested

- 1 bacteria. Engagement of macrophage apoptosis should be investigated as a novel host-
- 2 based antimicrobial strategy.
- 3

1 **Introduction**

2 Community-acquired pneumonia (CAP), commonly caused by *Streptococcus*
3 *pneumoniae* (the pneumococcus) and other bacteria, is a leading causes of global mortality
4 (1). The plasticity of bacterial genomes challenges vaccination and facilitates
5 antimicrobial resistance (2). Pathogenic bacteria frequently colonize the upper airway, but
6 CAP is relatively uncommon, indicating efficient host responses protect most individuals.

7
8 Tissue macrophages, such as alveolar macrophages (AM), are key effectors of
9 antibacterial host defense (3), but the mechanisms used to kill extracellular bacteria after
10 their internalization are incompletely defined. AM kill ingested bacteria in
11 phagolysosomes, but this mechanism is less efficient than in other phagocytes. Tissue
12 macrophages usually do not express myeloperoxidase (4) or the microbicidal serine
13 proteases seen in neutrophils (5) and are less reliant on nicotinamide adenine dinucleotide
14 phosphate (NADPH) oxidase-dependent reactive oxygen species (ROS) generation (6).
15 Nitric oxide (NO) generation in human macrophages is also less vigorous than in rodent
16 cells or monocytes (7, 8). Moreover, pneumococci and other bacterial pathogens
17 frequently express genes that inhibit phagolysosomal killing (9). Prolonged intracellular
18 killing of bacteria is associated with macrophage apoptosis in human macrophages and in
19 murine pneumonia models (3, 10). Although inhibition of apoptosis reduces bacterial
20 killing in these murine models it has not been demonstrated if cell-autonomous
21 macrophage apoptosis mediates pathogen clearance (3, 11). Recently we have found that
22 a key regulator of macrophage apoptosis during bacterial killing, the anti-apoptotic protein
23 Mcl-1 (11), is upregulated in AM from patients at increased risk of CAP due to chronic
24 obstructive pulmonary disease (COPD) or HIV-1 infection, where it is associated with
25 reduced AM apoptosis and bacterial killing ex vivo (12, 13). Re-engaging microbicidal
26 responses downstream of apoptosis restored bacterial killing in COPD AM (12) but

1 whether apoptosis reconstitution in the presence of over-expression of Mcl-1 restores
2 bacterial killing is unknown.

3

4 To test if macrophage cell autonomous over-expression of the human Mcl-1 transgene, as
5 observed in these patients at increased risk of CAP, mediates bacterial clearance we
6 generated transgenic mice that specifically express CD68.hMcl-1 in macrophages, since
7 the viability of these cells is closely linked to expression of this anti-apoptotic protein (11,
8 14). We used this novel transgenic line with controlled infections and interventions to
9 define the role, microbicidal mechanism and potential for therapeutic re-engagement of
10 macrophage apoptosis-associated bacterial killing. Our findings show that macrophage
11 apoptosis represents a second late-phase of bacterial killing, which is activated after initial
12 lysosome-mediated mechanisms are exhausted upon sustained bacterial
13 uptake. Apoptosis-associated bacterial killing requires mitochondrial (mROS), which act
14 in combination with NO. This microbicidal mechanism was inhibited in the presence of
15 CD68.hMcl-1, but was restored by BH3 mimetics or bisphosphonates.

16

1 **Materials and Methods**

2 *Generation of CD68.hMcl-1 transgenic mice:* A 1.5kb fragment containing the cDNA
3 sequence for human Mcl-1 (15) was cloned into a plasmid containing 2.9 kb of the CD68
4 promoter with the first intron enhancer IVS (16) (Figure 1A). Correct orientation and
5 PCR mismatches were confirmed by sequencing. The transgene was isolated by restriction
6 enzyme digestion and gel purification. The transgene was microinjected into C57Bl/6J
7 oocytes (Washington University School of Medicine, St Louis, USA). Founders and their
8 progeny were genotyped by PCR amplification of tail or ear biopsy DNA using the
9 following primers: 5'-ACCATCTCCTCTCTGCCAAA-3' and 5'-
10 GGGCTTCCATCTCCTCAA-3'. Two CD68.hMcl-1 mice transgenic lines were
11 established. Both lines showed germline transmission and equivalent functional results.
12 Mcl-1 transgenic mice and non-transgenic littermates, from the same cages, were
13 inoculated with bacteria and sample collected as described previously (3) and in the on-
14 line supplement.

15

16 *Bacteria:* Details on the bacteria and culture conditions are provided on-line.

17

18 *Isolation and culture of macrophages and other leukocytes:* Bone marrow-derived
19 macrophages (BMDM), resident AM , peritoneal macrophages (PM), peripheral blood
20 neutrophils, B-cells and T-cells were obtained from C57Bl/6J mice (17, 18). Human
21 monocyte-derived macrophages (MDM) from whole blood donated by healthy volunteers
22 (10). Further details are available on-line.

23

1 Flow Cytometry and confocal microscopy: Further details on flow cytometry and confocal
2 microscopy experiments are available in the on-line supplement.

3

4 *Intracellular killing assay:* Assessment of intracellular bacterial viability was carried out
5 as previously described (19), and outlined in the on-line supplement.

6

7 *Reconstitution of Apoptosis:* Apoptosis was reconstituted in vitro with clodronate-
8 encapsulated liposomes or the indicated BH3 mimetics and in vivo AM apoptosis was
9 reconstituted in transgenic mice using clodronate containing liposomes or the indicated
10 BH3 mimetics (further information in the on-line supplement), with instillation of bacteria
11 at the same time to ensure induction of early-stage apoptosis but not macrophage depletion
12 (20).

13

14 *Ethics:* Animal experiments were conducted in accordance with the Home Office
15 Animals (Scientific Procedures) Act of 1986, authorized under a UK Home Office
16 License 40/3251 with approval of the Sheffield Ethical Review Committee. MDM were
17 isolated from healthy volunteers with written informed consent and approval from the
18 South Sheffield Regional Ethics Committee.

19

20 *Statistics:* Results are recorded as mean and SEM. Sample sizes were informed by
21 standard errors obtained from similar assays in prior publications (10, 11). D'Agostino-
22 Pearson normality tests guided test selection. Comparisons between two conditions were
23 performed using a paired or unpaired t-test for parametric data, or a Mann-Whitney U test
24 or Wilcoxon signed rank test for non-parametric data using Prism 6.0 software (GraphPad
25 Inc.). Comparisons between three or more conditions were performed using a normal or

1 repeated measures 1-way ANOVA with Bonferroni post-test for parametric data, or a
2 Friedman test with Dunn's multiple comparison post-test for non-parametric data. When
3 two or more conditions were assessed in two experimental groups data was analysed by
4 2-way ANOVA with Bonferroni post-test. Significance was defined as $P < 0.05$.

5

Results

CD68.hMcl-1 transgenic mice demonstrate reduced macrophage apoptosis

A CD68 promoter construct (21) ensured macrophage-specific human Mcl-1 (hMcl-1) expression, to generate a transgenic mouse with selective apoptosis resistance in macrophages (Figure 1A). Equivalent functional results were generated from both founder lines. Macrophage-specific hMcl-1 expression was documented in AM and other macrophage lineages in CD68.hMcl-1 transgenic mice (Figure 1B-D), but not neutrophils or lymphocytes (Figure 1E). CD68.hMcl-1 transgenic mice lacked a gross developmental phenotype or loss of fertility and showed normal survival. CD68.hMcl-1 mice had normal numbers of leukocyte subsets in blood and of macrophage in tissues, while splenic lymphoid tissue and lung parenchyma showed no histological abnormalities (Figure E1A-F).

Importantly, the transgene reduced susceptibility to apoptosis in bone marrow-derived macrophages, (CD68.hMcl-1⁺ BMDM), AM and peritoneal macrophages (Figure 1F-H and E1G). In contrast, CD68.hMcl-1⁺ BMDM demonstrated no decrease in binding or ingestion of latex beads or in the numbers of viable intracellular bacteria present after 4 h exposure to *S. pneumoniae* (a marker of early ingestion and killing (10)) (Figure E1H-I). The generation of ROS and NO was also unaltered by the transgene at 4 h (Figure E1J-K). Mcl-1 thus did not alter initial innate immune responses.

Mcl-1 expression regulates apoptosis-associated killing when phagolysosomal bacterial killing is exhausted

Exposure of macrophages to pneumococci for 16-20 h results in apoptosis without a loss of membrane integrity (22). Importantly, this was inhibited in the presence of the

CD68.hMcl-1 transgene, which acted at the level of the mitochondrial execution of the program of apoptosis (Figure E2A-D). The transgene also increased survival of ingested bacteria (Figure 2A), although it had no effect on lysosomal acidification, lysosomal membrane permeabilization, or activation of the lysosomal protease cathepsin D, which occurs upstream of the mitochondrial apoptotic program following pneumococcal challenge (11, 14) (Figure E2E-G). To prove that reduction of macrophage apoptosis was the mechanism by which Mcl-1 inhibited bacterial killing, apoptosis was reconstituted with the BH3 mimetic ABT-737. Although ABT-737 cannot reverse the anti-apoptotic effect of Mcl-1 directly, it interacts with Bcl-2/Bcl-X_L, displacing pro-apoptotic Bcl-2 proteins to stimulate apoptosis (23). ABT-737 increased the number of cells with loss of inner mitochondrial transmembrane potential ($\Delta\psi_m$) and nuclear fragmentation in CD68.hMcl-1⁺ BMDM exposed to pneumococci (Figure E3A-B), and restored apoptosis-associated intracellular bacterial killing (Figure 2B), while additional BH3 mimetics also increased bacterial killing at 20 h, but not at 4 h (Figure E3C-D).

To dissect the role of apoptosis-associated killing in host defense, BMDM were ‘pulsed’ with bacteria and the kinetics of killing of internalized bacteria were measured following antimicrobial ‘chase’ to remove extracellular bacteria. The ‘chase’ does not itself alter internalized bacteria since the cell membrane remains intact at this early-stage of apoptosis (22) and ensures that changes in viable bacteria are the result of intracellular killing but not continued phagocytosis. We identified two phases of intracellular killing. An initial-phase, occurring immediately after bacterial ingestion (Figure 2C), was consistent with phagocytosis-associated phagolysosomal killing (24) and was similar in transgenic and non-transgenic BMDM. A late-phase of intracellular killing occurred at 16-20 h in non-transgenic BMDM but was blunted in CD68.hMcl-1⁺ BMDM. This late-phase coincided with the onset of apoptosis (Figure 2D) but occurred prior to any

1 reduction in macrophage cell numbers (Figure 2E). By varying the duration of the ‘pulse’
2 we confirmed that the initial phase of bacterial killing was sustained for up to 12 h and
3 that, after it ceased, the late-phase of killing cleared viable internalized bacteria (Figure
4 2F). Overall, the CD68.hMcl-1 transgene inhibited the late-phase of bacterial killing
5 without any impact on early ingestion or killing.

6

7 We tested whether bacterial ingestion was compromised after ≥ 12 h of exposure to
8 bacteria, as this would remove the stimulus for phagolysosomal killing. We investigated
9 this using a second ‘pulse’ with a distinct strain of bacteria (Figure 2G). Bacterial
10 internalization occurred at ≥ 12 h in the presence or absence of the Mcl-1 transgene, but
11 was accompanied by continued intracellular killing only in CD68.hMcl-1⁻ BMDM.
12 Sustained bacterial ingestion activated a late-phase of killing, requiring apoptosis
13 induction, killing viable internalized bacteria.

14

15 *Mitochondrial ROS is required for apoptosis-associated bacterial killing*

16 An inhibitor of nitric oxide synthase (NOS) 2 reduced both the late-phase of bacterial
17 killing and apoptosis in non-transgenic BMDM (Figure 3A-B). This suggested that NO
18 generation contributed to bacterial killing, but occurred upstream of apoptosis, consistent
19 with its known role in sensitizing mitochondria to apoptosis induction (19). An antioxidant
20 also inhibited late-phase bacterial killing, although it did not affect apoptosis-induction.
21 This suggested that ROS are also required for this phase, but are generated downstream
22 or as a result of apoptosis. Since NADPH oxidase does not contribute to macrophage
23 apoptosis-associated killing during pneumococcal infection (25), we addressed another
24 source of antimicrobial ROS, mitochondrial ROS (mROS) (26).

25

1 Increased mROS were apparent after 16-20 h of bacterial exposure, but were reduced by
2 the Mcl-1 transgene (Figure 3C). Peak generation of mROS co-incided with peak NO
3 production in human MDM (Figure E4A) and mROS/NO co-localized with bacteria
4 (Figure E4-6). Since mROS generation was a late response contemporaneous with
5 apoptosis onset we tested whether caspase 3 activation, which inhibits mitochondrial
6 electron transport complex I and II, contributed to mROS generation (27). Caspase
7 activation increased mROS production and, consistent with the role of Mcl-1 in limiting
8 caspase activation, the caspase 3/7⁺ population was expanded in non-transgenic versus
9 transgenic BMDM and produced significantly more mROS after 20 h of exposure to
10 bacteria (Figure 3D). Comparable findings were observed in human MDM (Figure 3E).
11 Crucially, an inhibitor of mROS, mitoTEMPO, blocked the late-phase of pneumococcal
12 killing in CD68.hMcl-1⁻ (but not CD68.hMcl-1⁺) BMDM (Figure 3F) and also in human
13 MDM (Figure 3G). Inhibition of mROS did not modify BMDM apoptosis-induction or
14 Mcl-1 expression (Figure 3H and 3I), consistent with mROS acting downstream of
15 apoptosis in bacterial killing. Since mROS also activates pro-inflammatory cytokine
16 expression (28) we confirmed differential cytokine expression was not contributing to
17 differences in late microbicidal responses (Figure E7 A-C). Since pneumococci
18 intrinsically resist oxidative stress (29), our results suggest apoptosis-associated killing
19 requires caspase-dependent mROS generation, combined with NO, to mediate bacterial
20 killing

21 22 *Apoptosis-associated killing is required for bacterial clearance in vivo*

23 We next addressed the role of apoptosis-associated bacterial killing by AM *in vivo*.
24 Initially we used a low-dose of pneumococci which AM clear efficiently, an intermediate
25 dose, which represents the ‘tipping-point’ at which AM start to fail to control infection
26 and where any increase in dose or perturbation of macrophage function results in

development of pneumonia, and a high doses where AM are overwhelmed and mice develop systemic infection (3, 30). CD68.hMcl-1⁺ transgenic mice failed to clear the low dose of pneumococci (10⁴ colony forming units; CFU) by 24 h, while non-transgenic mice cleared all bacteria (Figure 4A) (3). Only transgenic mice developed bacteremia at the low dose (Figure 4B). At intermediate doses, CD68.hMcl-1⁺ transgenic mice also exhibited increased bacterial CFU in lungs and blood compared to non-transgenic mice. Crucially the transgenic mice had significant neutrophil recruitment in BAL at this intermediate dose, a feature of pneumonia, while the non-transgenic animals had no neutrophil recruitment (Figure 4C). AM numbers were not altered by low dose infection or transgene expression but were only reduced in the high dose infection in transgenic mice in association with high-levels of inflammatory cell recruitment (Figure 4D). The bacterial clearance that occurred in non-transgenic animals was completely overwhelmed as expected at an inoculum of 10⁷ CFU macrophages (3). Along with reduced bacterial clearance and an increased requirement for neutrophil recruitment, CD68.hMcl-1⁺ transgenic mice exhibited reduced AM apoptosis in bronchoalveolar lavage (BAL) following bacterial challenge (Figure 4E). To exclude any role for low numbers of lung neutrophils in the differential clearance of bacteria we repeated low dose bacterial challenge after neutrophil depletion and again confirmed reduced bacterial clearance in the transgenic mice (Figure E8). Overall this proved the transgene reduced bacterial replication and also the threshold at which neutrophils were recruited to control bacteria in the lung, but only during the specific stages where AM are the major effector of bacterial clearance in the lung.

CD68.hMcl-1⁺ transgenic mice also exhibited impaired clearance of low doses of *H. influenzae*, another respiratory pathogen (31). At high doses, infection progressed to pneumonia with pulmonary neutrophil recruitment in all mice, since AM clearance

1 capacity was overwhelmed (Figure 4F-G). Reduced bacterial clearance at low doses was
2 also associated with reduced macrophage apoptosis in the BAL (Figure 4H). Apoptosis-
3 associated killing likewise contributed to bacterial clearance at extra-pulmonary sites:
4 CD68.hMcl-1⁺ transgenic mice given a low peritoneal dose of *S. pneumoniae* showed
5 impaired peritoneal clearance of bacteria, increased numbers of bacteria in blood,
6 enhanced neutrophil numbers and reduced macrophage apoptosis (Figure 4I-L).

7

8 *Re-engagement of macrophage apoptosis enhances pulmonary bacterial clearance in vivo*

9 To confirm that the differential levels of apoptosis explained the transgene effect *in vivo*,
10 we reconstituted AM apoptosis in the CD68.hMcl-1⁺ transgenic mice using liposomes
11 containing clodronate (20). Liposomes ensure macrophage targeting through phagocytic
12 uptake, while clodronate induces a mitochondrial pathway of apoptosis with loss of $\Delta\psi_m$
13 providing an alternative route of engagement of the mitochondrial apoptosis pathway in
14 the absence of Mcl-1 downregulation (32, 33). Liposome dosing was adjusted to induce
15 apoptosis in CD68.hMcl-1⁺ BMDM exposed to bacteria (Figure 5A), without altering
16 bacterial internalization (Figure 5B). *In vivo* we administered liposomes at the same time
17 as bacteria, to ensure that the early stages of liposome-induced AM apoptosis occurred
18 together with the initiation of the anti-bacterial apoptotic program and before AM
19 depletion reduced AM numbers (Figure 5C and 5D). Reconstitution of AM apoptosis in
20 CD68.hMcl-1⁺ AM increased bacterial clearance from the lung, reduced levels of
21 bacteria in the blood, and reduced neutrophil numbers in BAL (Figure 5E-G). Similar
22 results were obtained with BH3 mimetics (ABT-263, an oral derivative of ABT-737 and
23 sabutoclax, a pan Bcl-2 family inhibitor (34)). These increased bacterial clearance from
24 lung and blood (Figure 5H-I) and AM apoptosis but not AM numbers, in infections
25 inducing minimal neutrophil recruitment (Figure E9). They also reduced viable bacteria
26 in MDM at late, but not early time-points (Figure E9D-E).

1

2 Adoptive transfer of bone marrow between non-transgenic and transgenic mice
3 confirmed our results reflected macrophage expression of the transgene. Bone marrow
4 transplantation reduces the ability of mice to clear the low dose of pneumococci (14, 35)
5 and bacteria were not completely cleared in either group of mice (Figure E10A-B).
6 However, the recipients of transgenic bone marrow exhibited reduced AM apoptosis and
7 greater numbers of macrophage-associated bacteria (consistent with reduced
8 intracellular clearance), while recruiting significantly more neutrophils (Figure E10C-E).
9 This suggested that there was less effective macrophage killing in transgenic mice.

10

11 *Staphylococcus aureus* infection does not activate apoptosis-associated killing

12 *Staphylococcus aureus* upregulates Mcl-1 in macrophages (36). We wondered whether
13 this would phenocopy the effects seen with the CD68.hMcl-1 transgene. Induction of
14 macrophage apoptosis requires downregulation of Mcl-1 to allow mitochondrial outer
15 membrane permeabilization (MOMP) and the execution phase of apoptosis (11, 14). *S.*
16 *aureus* failed to induce the anticipated Mcl-1 downregulation after sustained bacterial
17 ingestion (Figure E11A). Moreover, it was not associated with apoptosis or late-phase
18 bacterial killing (Figure 6A-B), despite exhaustion of the initial phase of killing in the
19 setting of sustained ingestion of bacteria (Figure 6C-D). Exposure *in vivo* to a range of
20 bacterial doses (from doses AM can control to 100-fold higher) did not reveal any
21 differences in bacterial clearance, neutrophil recruitment, or AM apoptosis irrespective of
22 transgene expression (Figure 6E-G). In contrast to pneumococcal infection, ABT-737
23 failed to enhance bacterial killing or to reconstitute apoptosis at the dose that induced
24 apoptosis in transgenic BMDM after pneumococcal challenge (Figure E11B-C). ABT-
25 737 was used to reconstitute apoptosis since it does not alter uptake, in contrast to

1 liposomes (3), in which altered phagocytosis can confound interpretation during high-
2 uptake phagocytosis, as seen with *S. aureus*. These findings highlight the importance of
3 apoptosis-associated killing as a mechanism subverted by some pathogens.

4

1 **Discussion:**

2 Development of a macrophage specific CD68.hMcl-1 transgenic mouse provided a unique
3 means of examining the role and mechanism of macrophage apoptosis-associated
4 bacterial killing in the lung. Use of this model identified a novel paradigm whereby
5 macrophage apoptosis kills internalized bacteria that remain viable after initial
6 phagolysosomal killing is exhausted. During apoptosis induction caspase-dependent
7 mROS production combines with NO to achieve a second late-phase of bacterial killing.
8 Inhibition of macrophage apoptosis by Mcl-1 increases susceptibility to bacterial infection
9 but can be modulated pharmacologically to enhance pulmonary bacterial clearance.

10

11 Macrophages' avid phagocytic capacity ensures intracellular loading with ingested
12 bacteria (37, 38). Phagocytosis activates an initial-phase of bacterial killing, consistent
13 with observations describing temporal association of the NOX2 complex with neutrophil
14 phagocytosis (24), but sustained phagocytosis overwhelms initial microbicidal responses.
15 A late-phase microbicidal response, during the initial stages of apoptosis, clears remaining
16 viable internalized bacteria. Macrophage apoptosis occurs during *M. tuberculosis*
17 infection (39), but also with other pulmonary micro-organisms, such as pneumococci,
18 unable to persist intracellularly, suggesting it limits intracellular persistence (11, 14).

19

20 Our approach, using macrophage specific transgene expression (16), allowed selective
21 modulation of the early stages of apoptosis via Mcl-1, with relative resistance to apoptosis,
22 which regulates macrophage survival following pneumococcal infection (11). Mcl-1 is
23 unique amongst anti-apoptotic Bcl-2 proteins because it is an early response gene with
24 rapid induction and turnover (40). Mcl-1 transgene expression in myeloid cells prolongs
25 macrophage survival but ensures sensitivity to physiological constraints on viability, and
26 that cell numbers remain within the normal range (15).

1

2 Emerging data in patients at risk of CAP show Mcl-1 upregulation in AM is associated
3 with reduced bacterial killing (12, 13). During HIV-1 infection gp120 inhibits Mcl-1
4 ubiquitination and proteasomal degradation while in COPD transcriptional upregulation
5 is associated with anti-oxidant responses during oxidative stress (12, 13) . In our murine
6 model over-expression of Mcl-1 using the human transgene converted low dose lung
7 infections, which macrophages normally control (3), into established infections inducing
8 neutrophilic inflammation, phenocopying the susceptibility of patient AM *ex vivo*. In
9 comparison with *S. pneumoniae* and *H. influenzae*, *S. aureus* is less readily killed by
10 differentiated macrophages (41) and internalized bacteria remain viable for several days
11 (42). *S. aureus* containing-phagosomes fail to mature appropriately, decreasing cathepsin
12 D activation required for Mcl-1 proteasomal degradation (14, 43). We show *S. aureus*
13 prevents apoptosis-associated killing, however unlike pneumococcal infection we could
14 not reconstitute apoptosis-associated killing following *S. aureus* infection. A potential
15 explanation for this finding could be that altered endosomal trafficking of *S. aureus* needs
16 to be corrected (43), to allow induction of apoptosis and to allow co-localization with
17 mitochondria to mediate microbicidal killing (26). Thus HIV, COPD and *S. aureus*
18 infection all inhibit bacterial killing by upregulating Mcl-1, similar to the over-expression
19 of the human Mcl-1 transgene in our murine model.

20

21 The relevance of animal models to human disease merits careful scrutiny. Murine
22 pneumonia models confirm roles for the key innate cell populations contributing to
23 pathogenesis in CAP and reprise the susceptibility of key single gene defects or
24 polymorphisms identified in humans, despite some differences in specific innate
25 responses (e.g. extent of reliance on NOS2 (inducible NO synthase) in macrophages, α -
26 defensin expression in neutrophils or activation patterns following specific Toll-like

1 receptor ligands) (44). The C57Bl/6 strain has intermediate susceptibility to pneumococci
2 (45) and inocula can be adapted to favour AM-dependent clearance or sequential
3 requirement of T-cells and recruited neutrophils in this model (30). They also show
4 evidence of AM apoptosis (3) and increased susceptibility to pneumococcal disease
5 following Mcl-1 over-expression (11). A murine model allowed us to test the impact of
6 genetic modulation of Mcl-1 *in vivo* in the context of early stage sub-clinical infection,
7 something not possible in patients who present at the later stage of established disease.
8 Impaired clearance of pneumococci in association with Mcl-1 upregulation in patient
9 groups at increased risk of CAP suggests these finding are relevant to human disease.
10 Moreover, we demonstrated key mechanistic requirements for caspase-dependent mROS,
11 combined with NO, in apoptosis-associated killing in human MDM, as well as increased
12 bacterial clearance with BH3 mimetics.

13
14 Apoptosis-associated bacterial killing requires mROS, a recently identified microbicidal
15 (26). During apoptosis execution caspase 3, inhibits mitochondrial electron transport
16 complexes I and II (27), resulting in in generation of superoxide (46). SOD2 upregulation
17 during pneumococcal infection prevents necroptosis (47, 48) ensuring mitochondrial
18 permeabilization is limited in extent, a specific feature of apoptosis (11, 14, 48, 49).
19 However, antioxidant protection does not extend to the immediate environment of the
20 phagolysosome, permitting microbial killing (26). Pneumococcal anti-oxidant systems
21 protect against NADPH-dependent ROS generation in neutrophils (9). Our results,
22 however, suggest that peak mROS and NO co-exist, consistent with the role of NO in the
23 late microbicidal macrophage response (19, 25). Potential sources of NO include NOS2
24 but also NOS3 (endothelial NOS), which contributes to AM microbicidal responses to
25 pneumococci (50) and mitochondria which generate NO through NOS-independent and
26 NOS-dependent mechanisms (including the debated existence of an inner membrane-

1 associated or matrix isoform) (51). Cross-reactivity of inhibitors between isoforms and
2 residual controversies concerning NOS2 in humans means the source of NO requires
3 further clarification. We propose a model where mROS and NO generation is temporally
4 and spatially linked, and co-localizes with bacteria containing phagolysosomes as
5 previously shown (19), allowing generation of reactive nitrogen species (RNS). We did
6 not identify NO regulation by mROS, since mROS occurred downstream of Mcl-1-
7 mediated apoptosis regulation, while NO production was upstream and unaltered by the
8 Mcl-1 transgene. NO and RNS can, however, enhance mROS generation (51). We found
9 no evidence that mROS role in killing was mediated by differential cytokine expression.
10 While mROS can induce pro-inflammatory cytokine expression (28), during the early
11 stages of bacterial-associated apoptosis induction protein translation is reduced, limiting
12 this possibility (36).

13
14 Since we demonstrate a critical role for apoptosis-associated killing in mediating bacterial
15 clearance by macrophages, it follows that upregulation of Mcl-1 influences susceptibility
16 to bacterial pneumonia. The use of a murine model in which we could alter Mcl-1
17 expression through transgene expression and deliver controlled infections and
18 pharmacological interventions allowed us to confirm the role and mechanisms of this
19 process to an extent not possible with our prior studies in patients (12, 13). Our data
20 suggests that susceptibility to bacterial infection can be reversed through therapeutic
21 targeting of the mitochondrial-microbicidal axis or modulation of Mcl-1. Several classes
22 of therapeutics, including bisphosphonates and BH3 mimetics, target these pathways (20,
23 23). As proof of concept of this repurposing approach ABT737 has recently demonstrated
24 utility in preventing intracellular replication of *Legionella pneumophila* in AM through
25 induction of apoptosis (52). We also demonstrated Bcl-2 specific and pan-Bcl-2 inhibitors
26 enhanced pneumococcal clearance, with more significant results demonstrated for

1 sabutoclax an agent that inhibits Mcl-1 (53). However, for some pathogens like *S. aureus*
2 the strategy may need to be adapted to reverse altered endosomal trafficking (43). In view
3 of the on-going therapeutic challenge of antimicrobial resistance, re-engaging this
4 fundamental microbicidal mechanism in AM merits further evaluation.

5

6

7

8

9 **Disclosure of Conflicts of Interest**

10 All authors have declared that no competing financial interests exist.

References

1. O'Brien KL, Wolfson LJ, Watt JP, Henkle E, Deloria-Knoll M, McCall N, Lee E, Mulholland K, Levine OS, Cherian T. Burden of disease caused by *Streptococcus pneumoniae* in children younger than 5 years: global estimates. *Lancet* 2009; 374: 893-902.
2. Croucher NJ, Harris SR, Fraser C, Quail MA, Burton J, van der Linden M, McGee L, von Gottberg A, Song JH, Ko KS, Pichon B, Baker S, Parry CM, Lambertsen LM, Shahinas D, Pillai DR, Mitchell TJ, Dougan G, Tomasz A, Klugman KP, Parkhill J, Hanage WP, Bentley SD. Rapid pneumococcal evolution in response to clinical interventions. *Science* 2011; 331: 430-434.
3. Dockrell DH, Marriott HM, Prince LR, Ridger VC, Ince PG, Hellewell PG, Whyte MK. Alveolar macrophage apoptosis contributes to pneumococcal clearance in a resolving model of pulmonary infection. *J Immunol* 2003; 171: 5380-5388.
4. Cohen AB, Cline MJ. The human alveolar macrophage: isolation, cultivation in vitro, and studies of morphologic and functional characteristics. *J Clin Invest* 1971; 50: 1390-1398.
5. Jin M, Opalek JM, Marsh CB, Wu HM. Proteome comparison of alveolar macrophages with monocytes reveals distinct protein characteristics. *American journal of respiratory cell and molecular biology* 2004; 31: 322-329.
6. Kobzik L, Godleski JJ, Brain JD. Oxidative metabolism in the alveolar macrophage: analysis by flow cytometry. *Journal of leukocyte biology* 1990; 47: 295-303.
7. Jesch NK, Dorger M, Enders G, Rieder G, Vogelmeier C, Messmer K, Krombach F. Expression of inducible nitric oxide synthase and formation of nitric oxide by alveolar macrophages: an interspecies comparison. *Environ Health Perspect* 1997; 105 Suppl 5: 1297-1300.
8. Daigneault M, Preston JA, Marriott HM, Whyte MK, Dockrell DH. The identification of markers of macrophage differentiation in PMA-stimulated THP-1 cells and monocyte-derived macrophages. *PLoS One* 2010; 5: e8668.
9. Aberdein JD, Cole J, Bewley MA, Marriott HM, Dockrell DH. Alveolar macrophages in pulmonary host defence the unrecognized role of apoptosis as a mechanism of intracellular bacterial killing. *Clin Exp Immunol* 2013; 174: 193-202.
10. Dockrell DH, Lee M, Lynch DH, Read RC. Immune-mediated phagocytosis and killing of *Streptococcus pneumoniae* are associated with direct and bystander macrophage apoptosis. *J Infect Dis* 2001; 184: 713-722.
11. Marriott HM, Bingle CD, Read RC, Braley KE, Kroemer G, Hellewell PG, Craig RW, Whyte MK, Dockrell DH. Dynamic changes in Mcl-1 expression regulate macrophage viability or commitment to apoptosis during bacterial clearance. *J Clin Invest* 2005; 115: 359-368.
12. Bewley MA, Preston JA, Mohasin M, Marriott HM, Budd RC, Swales J, Collini P, Greaves DR, Craig RW, Brightling CE, Donnelly LE, Barnes PJ, Singh D, Shapiro SD, Whyte MKB, Dockrell DH. Impaired Mitochondrial Microbicidal Responses in Chronic Obstructive Pulmonary Disease Macrophages. *Am J Respir Crit Care Med* 2017; 196: 845-855.
13. Collini PJ, Bewley MA, Mohasin M, Marriott HM, Miller RF, Geretti AM, Beloukas A, Papadimitropoulos A, Read RC, Noursadeghi M, Dockrell DH. HIV gp120 in the Lungs of Antiretroviral Therapy-treated Individuals Impairs Alveolar Macrophage Responses to Pneumococci. *Am J Respir Crit Care Med* 2018; 197: 1604-1615.
14. Bewley MA, Marriott HM, Tulone C, Francis SE, Mitchell TJ, Read RC, Chain B, Kroemer G, Whyte MK, Dockrell DH. A cardinal role for cathepsin d in co-

- ordinating the host-mediated apoptosis of macrophages and killing of pneumococci. *PLoS pathogens* 2011; 7: e1001262.
15. Zhou P, Qian L, Bieszczad CK, Noelle R, Binder M, Levy NB, Craig RW. Mcl-1 in transgenic mice promotes survival in a spectrum of hematopoietic cell types and immortalization in the myeloid lineage. *Blood* 1998; 92: 3226-3239.
16. Gough PJ, Gordon S, Greaves DR. The use of human CD68 transcriptional regulatory sequences to direct high-level expression of class A scavenger receptor in macrophages in vitro and in vivo. *Immunology* 2001; 103: 351-361.
17. Shipley JM, Wesselschmidt RL, Kobayashi DK, Ley TJ, Shapiro SD. Metalloelastase is required for macrophage-mediated proteolysis and matrix invasion in mice. *Proc Natl Acad Sci U S A* 1996; 93: 3942-3946.
18. Cotter MJ, Norman KE, Hellewell PG, Ridger VC. A novel method for isolation of neutrophils from murine blood using negative immunomagnetic separation. *Am J Pathol* 2001; 159: 473-481.
19. Marriott HM, Ali F, Read RC, Mitchell TJ, Whyte MK, Dockrell DH. Nitric oxide levels regulate macrophage commitment to apoptosis or necrosis during pneumococcal infection. *The FASEB journal : official publication of the Federation of American Societies for Experimental Biology* 2004; 18: 1126-1128.
20. Van Rooijen N, Sanders A. Liposome mediated depletion of macrophages: mechanism of action, preparation of liposomes and applications. *J Immunol Methods* 1994; 174: 83-93.
21. Greaves DR, Quinn CM, Seldin MF, Gordon S. Functional comparison of the murine macrosialin and human CD68 promoters in macrophage and nonmacrophage cell lines. *Genomics* 1998; 54: 165-168.
22. Bewley MA, Naughton M, Preston J, Mitchell A, Holmes A, Marriott HM, Read RC, Mitchell TJ, Whyte MK, Dockrell DH. Pneumolysin activates macrophage lysosomal membrane permeabilization and executes apoptosis by distinct mechanisms without membrane pore formation. *MBio* 2014; 5: e01710-01714.
23. van Delft MF, Huang DC. How the Bcl-2 family of proteins interact to regulate apoptosis. *Cell Res* 2006; 16: 203-213.
24. DeLeo FR, Allen LA, Apicella M, Nauseef WM. NADPH oxidase activation and assembly during phagocytosis. *J Immunol* 1999; 163: 6732-6740.
25. Marriott HM, Hellewell PG, Whyte MK, Dockrell DH. Contrasting roles for reactive oxygen species and nitric oxide in the innate response to pulmonary infection with *Streptococcus pneumoniae*. *Vaccine* 2007; 25: 2485-2490.
26. West AP, Brodsky IE, Rahner C, Woo DK, Erdjument-Bromage H, Tempst P, Walsh MC, Choi Y, Shadel GS, Ghosh S. TLR signalling augments macrophage bactericidal activity through mitochondrial ROS. *Nature* 2011; 472: 476-480.
27. Ricci JE, Gottlieb RA, Green DR. Caspase-mediated loss of mitochondrial function and generation of reactive oxygen species during apoptosis. *J Cell Biol* 2003; 160: 65-75.
28. Bulua AC, Simon A, Maddipati R, Pelletier M, Park H, Kim KY, Sack MN, Kastner DL, Siegel RM. Mitochondrial reactive oxygen species promote production of proinflammatory cytokines and are elevated in TNFR1-associated periodic syndrome (TRAPS). *J Exp Med* 2011; 208: 519-533.
29. Yesilkaya H, Andisi VF, Andrew PW, Bijlsma JJ. *Streptococcus pneumoniae* and reactive oxygen species: an unusual approach to living with radicals. *Trends Microbiol* 2013; 21: 187-195.
30. Marriott HM, Daigneault M, Thompson AA, Walmsley SR, Gill SK, Witcher DR, Wroblewski VJ, Hellewell PG, Whyte MK, Dockrell DH. A decoy receptor 3

- analogue reduces localised defects in phagocyte function in pneumococcal pneumonia. *Thorax* 2012; 67: 985-992.
31. King P. Haemophilus influenzae and the lung (Haemophilus and the lung). *Clin Transl Med* 2012; 1: 10.
 32. Lehenkari PP, Kellinsalmi M, Napankangas JP, Ylitalo KV, Monkkonen J, Rogers MJ, Azhayeve A, Vaananen HK, Hassinen IE. Further insight into mechanism of action of clodronate: inhibition of mitochondrial ADP/ATP translocase by a nonhydrolyzable, adenine-containing metabolite. *Mol Pharmacol* 2002; 61: 1255-1262.
 33. van Rooijen N, Sanders A, van den Berg TK. Apoptosis of macrophages induced by liposome-mediated intracellular delivery of clodronate and propamidine. *J Immunol Methods* 1996; 193: 93-99.
 34. Bajwa N, Liao C, Nikolovska-Coleska Z. Inhibitors of the anti-apoptotic Bcl-2 proteins: a patent review. *Expert Opin Ther Pat* 2012; 22: 37-55.
 35. Ojielo CI, Cooke K, Mancuso P, Standiford TJ, Olkiewicz KM, Clouthier S, Corrion L, Ballinger MN, Toews GB, Paine R, 3rd, Moore BB. Defective phagocytosis and clearance of *Pseudomonas aeruginosa* in the lung following bone marrow transplantation. *J Immunol* 2003; 171: 4416-4424.
 36. Koziel J, Maciag-Gudowska A, Mikolajczyk T, Bzowska M, Sturdevant DE, Whitney AR, Shaw LN, DeLeo FR, Potempa J. Phagocytosis of *Staphylococcus aureus* by macrophages exerts cytoprotective effects manifested by the upregulation of antiapoptotic factors. *PLoS One* 2009; 4: e5210.
 37. Steinman RM, Mellman IS, Muller WA, Cohn ZA. Endocytosis and the recycling of plasma membrane. *The Journal of cell biology* 1983; 96: 1-27.
 38. Cohn ZA, Fedorko ME, Hirsch JG. The in vitro differentiation of mononuclear phagocytes. V. The formation of macrophage lysosomes. *J Exp Med* 1966; 123: 757-766.
 39. Keane J, Balcewicz-Sablinska MK, Remold HG, Chupp GL, Meek BB, Fenton MJ, Kornfeld H. Infection by *Mycobacterium tuberculosis* promotes human alveolar macrophage apoptosis. *Infect Immun* 1997; 65: 298-304.
 40. Yang T, Kozopas KM, Craig RW. The intracellular distribution and pattern of expression of Mcl-1 overlap with, but are not identical to, those of Bcl-2. *The Journal of cell biology* 1995; 128: 1173-1184.
 41. Jonsson S, Musher DM, Chapman A, Goree A, Lawrence EC. Phagocytosis and killing of common bacterial pathogens of the lung by human alveolar macrophages. *J Infect Dis* 1985; 152: 4-13.
 42. Kubica M, Guzik K, Koziel J, Zarebski M, Richter W, Gajkowska B, Golda A, Maciag-Gudowska A, Brix K, Shaw L, Foster T, Potempa J. A potential new pathway for *Staphylococcus aureus* dissemination: the silent survival of *S. aureus* phagocytosed by human monocyte-derived macrophages. *PLoS One* 2008; 3: e1409.
 43. Jubrail J, Morris P, Bewley MA, Stoneham S, Johnston SA, Foster SJ, Peden AA, Read RC, Marriott HM, Dockrell DH. Inability to sustain intraphagolysosomal killing of *Staphylococcus aureus* predisposes to bacterial persistence in macrophages. *Cell Microbiol* 2016; 18: 80-96.
 44. Mizgerd JP, Skerrett SJ. Animal models of human pneumonia. *Am J Physiol Lung Cell Mol Physiol* 2008; 294: L387-398.
 45. Gingles NA, Alexander JE, Kadioglu A, Andrew PW, Kerr A, Mitchell TJ, Hopes E, Denny P, Brown S, Jones HB, Little S, Booth GC, McPheat WL. Role of genetic resistance in invasive pneumococcal infection: identification and study of

- susceptibility and resistance in inbred mouse strains. *Infect Immun* 2001; 69: 426-434.
46. Cai J, Jones DP. Superoxide in apoptosis. Mitochondrial generation triggered by cytochrome c loss. *J Biol Chem* 1998; 273: 11401-11404.
47. Galluzzi L, Kroemer G. Necroptosis: a specialized pathway of programmed necrosis. *Cell* 2008; 135: 1161-1163.
48. Bewley MA, Pham TK, Marriott HM, Noirel J, Chu HP, Ow SY, Ryazanov AG, Read RC, Whyte MK, Chain B, Wright PC, Dockrell DH. Proteomic evaluation and validation of cathepsin D regulated proteins in macrophages exposed to *Streptococcus pneumoniae*. *Molecular & cellular proteomics : MCP* 2011; 10: M111 008193.
49. Golstein P, Kroemer G. Cell death by necrosis: towards a molecular definition. *Trends in biochemical sciences* 2007; 32: 37-43.
50. Yang Z, Huang YC, Koziel H, de Crom R, Ruetten H, Wohlfart P, Thomsen RW, Kahlert JA, Sorensen HT, Jozefowski S, Colby A, Kobzik L. Female resistance to pneumonia identifies lung macrophage nitric oxide synthase-3 as a therapeutic target. *Elife* 2014; 3.
51. Lacza Z, Pankotai E, Busija DW. Mitochondrial nitric oxide synthase: current concepts and controversies. *Front Biosci (Landmark Ed)* 2009; 14: 4436-4443.
52. Speir M, Lawlor KE, Glaser SP, Abraham G, Chow S, Vogrin A, Schulze KE, Schuelein R, O'Reilly LA, Mason K, Hartland EL, Lithgow T, Strasser A, Lessene G, Huang DCS, Vince JE, Naderer T. Eliminating *Legionella* by inhibiting BCL-XL to induce macrophage apoptosis. *Nature Microbiology* 2016; 1.
53. Dash R, Azab B, Quinn BA, Shen X, Wang XY, Das SK, Rahmani M, Wei J, Hedvat M, Dent P, Dmitriev IP, Curiel DT, Grant S, Wu B, Stebbins JL, Pellecchia M, Reed JC, Sarkar D, Fisher PB. Apogossypol derivative BI-97C1 (Sabutoclax) targeting Mcl-1 sensitizes prostate cancer cells to mda-7/IL-24-mediated toxicity. *Proc Natl Acad Sci U S A* 2011; 108: 8785-8790.

Figure Legends

Figure 1: Macrophages from CD68.hMcl-1 transgenic mice express hMcl-1 and have selective resistance to apoptosis.

(A) Schematic representation of the transgene construct. Human Mcl-1 (hMcl-1) expression is driven in macrophages by 2.9 kb of the CD68 promoter and Intron 1 (IVS-1). (B-D) Western blot analysis of human (h) and murine (m) Mcl-1 protein expression in (B) bone marrow-derived macrophages (BMDM), (C) alveolar, and (D) peritoneal macrophages, from CD68.hMcl-1 non-transgenic (non-Tg) or transgenic (Tg) mice. (E) Peripheral blood neutrophils and splenic CD19⁺ B-lymphocytes (CD19⁺) or CD3⁺ T-lymphocytes (CD3⁺) were isolated from non-Tg or Tg mice. Cells were lysed and probed by western blot for human (h) Mcl-1 protein expression. Blots representative of three independent experiments. The +ve control is human monocyte-derived macrophage lysate. (F-G) BMDM from non-Tg or Tg mice were irradiated with UV radiation and assessed for (F) nuclear fragmentation at the indicated time-points, n=4, ***= p<0.001, 2-way ANOVA, or (G) caspase 3/7 activation measuring relative luminescence units (RLU) at 8h, n=4, *= p<0.05, 2-way ANOVA. Data are represented as mean ±SEM. (H) Alveolar (AM) macrophages from non-Tg or Tg mice were left untreated (negative), or UV treated. 8 h after UV exposure, apoptosis was assessed by nuclear fragmentation, n=4-5, ***= p<0.001 2-way ANOVA. Data are represented as mean ±SEM. See also Figure E1.

Figure 2: Apoptosis-associated killing ensures intracellular bacterial clearance when canonical phagolysosomal killing is exhausted.

(A) Bone marrow-derived macrophages (BMDM) from CD68.hMcl-1 non-transgenic (non-Tg) or transgenic (Tg) mice were mock-infected (MI) or challenged with serotype 2 *S. pneumoniae* (Spn) at a multiplicity of infection (MOI) of 10 and intracellular colony

forming units (CFU) assessed 20 h after infection, n=18, **= p<0.01, unpaired Student's t-test. (B) Non-Tg or Tg BMDM were challenged with Spn in the presence (+) or absence (-) of ABT-737. 20 h post-challenge cells were assessed for intracellular CFU, n=9, ***= p<0.001, 2-way ANOVA. (C) Non-Tg or Tg BMDM were challenged with Spn at MOI of 10 for 4 h and extracellular bacteria removed ('pulse-chase' design). BMDM were lysed for initial assessment of CFU or incubated in vancomycin until the designated time point when CFU were also determined, n=4, **= p<0.01, 2-way ANOVA. (D-E) BMDM were challenged with Spn at MOI of 10. At the designated time post-challenge, levels of apoptosis, (D), and the average number of cells per field (E), were measured, n=4, *= p<0.05, 2-way ANOVA. (F) Non-Tg or Tg BMDM were challenged with Spn at MOI of 10 for varying times before extracellular bacteria were killed and intracellular CFU estimated immediately or after a further 2 h incubation to measure intracellular killing capacity, n=4, **= p<0.01, 2-way ANOVA. (G) Non-Tg or Tg BMDM were challenged with Spn at MOI of 10 for varying intervals before extracellular bacteria were killed and cultures split, and one group were 'pulsed' with streptomycin resistant Spn (FP58) for 2 h, after which the intracellular CFU of FP58 were estimated as a marker of recent ingestion, n=5. Data are represented as mean \pm SEM. See also Figures E2-3.

Figure 3. Mcl-1 regulates caspase-induced late-phase mitochondrial ROS production.

(A-B) Bone marrow-derived macrophages (BMDM) from CD68.hMcl-1 non-transgenic (non-Tg) or transgenic (Tg) mice were challenged with serotype 2 *Streptococcus pneumoniae* (Spn) at a multiplicity of infection (MOI) of 10 in the presence (+) or absence of the antioxidant Trolox, or an iNOS inhibitor (1400W). (A) Intracellular bacterial colony forming units (CFU) were estimated 16 h post-challenge, n=5, or (B) nuclear

fragmentation was recorded 20 h post-challenge, n=6, **= p<0.01, 1-way or 2-way ANOVA for analyses within or between groups respectively. (C) Non-Tg or Tg BMDM were mock-infected (MI) or challenged with Spn at MOI of 10. At the indicated times post-challenge cells were stained with MitoSOX and analysed by flow cytometry. n=3 *= p<0.05, Students t-test. (D) Non-Tg or Tg BMDM were MI or challenged with Spn at MOI of 10. At the designated time points, cells were stained for mROS and caspase 3/7 activity by flow cytometry. Cells were selected by forward/side scatter (grey contour plots), before being designated as caspase negative or positive (green contour plots). MitoSox red staining was assessed for each caspase subpopulation and cell populations as a whole (histograms). Representative plots are shown, with collated data in the graph below, n=3 *= p<0.05, 2-way ANOVA. (E) Experiments in D were repeated in human MDM, n=4 *= p<0.05, 1-way ANOVA. (F-G) Non-Tg or Tg BMDM (F) or human MDM (G) were challenged with Spn at MOI of 10, in the presence or absence (vehicle) of mitoTEMPO (mT), 1400W, or a combination of both (Combo). 16 h post-challenge intracellular CFU were assessed, n=5 (for F) and n=8 (for G), *= p<0.05, **= p<0.01, repeated measures 1-way ANOVA (for F), or Friedman test (for G). (H-I) BMDM from non-Tg or Tg mice were MI or challenged with Spn at MOI of 10 in the presence (+) or absence (-) of mT. 20 h post-challenge cells were assessed by nuclear morphology (H), n=3, *= p<0.05, **= p<0.01, 2-way ANOVA, or (I) lysates were probed for human (h) and murine (m) Mcl-1 expression by western blot and densitometry performed on three independent experiments. Data are represented as mean \pm SEM. See also Figures E4-7.

Figure 4. Apoptosis-associated killing mediates bacterial clearance *in vivo*.

(A-E) CD68.hMcl-1 non-transgenic (non-Tg) or transgenic (Tg) mice were challenged with the designated dose of serotype 1 *Streptococcus pneumoniae* (Spn). 24 h after

1 instillation, bacterial colony forming units (CFU) in the lung homogenate (A) or blood
2 (B), the number of polymorphonuclear leukocytes (PMN) (C), the number of alveolar
3 macrophages (AM) (D), or the percentage of apoptotic AM (E) in the bronchoalveolar
4 lavage (BAL) were measured, n=4-11 mice per group from three independent
5 experiments, *= p<0.05 **= p<0.01, 2-way ANOVA. **(F-H)** Non-Tg and Tg mice were
6 challenged with *H. influenzae* type b (Hib) at the designated dose. 24 h after instillation,
7 CFU in the lung homogenate (F), PMN numbers in the BAL (G), and AM apoptosis (H),
8 were measured, n=4-13 mice per group, from 2 independent experiments, ***= p<0.001,
9 2-way ANOVA. **(I-L)** Non-Tg or Tg mice were challenged with the designated dose of
10 Spn intra-peritoneally. 24 h after challenge, the bacterial CFU in the peritoneal lavage
11 (PL) (I), n=7, or blood (J), were determined, n=7, and PMN numbers (K), n=7 and levels
12 of peritoneal macrophage (PM) apoptosis (L), n=9, in the PL were assessed by
13 microscopy. In all experiments, *= p<0.05, **= p<0.01, 2-way ANOVA. See also Figure
14 E8.

15

16 **Figure 5: Apoptosis-associated killing can be reconstituted following challenge with**
17 ***Streptococcus pneumoniae***

18 **(A)** Bone marrow-derived macrophages (BMDM) from CD68.hMcl-1 non-transgenic
19 (non-Tg) or transgenic (Tg) mice were challenged with liposomes containing PBS (LIPO-
20 PBS) or clodronate (LIPO-CLOD). At the designated time-point cells were fixed and
21 analysed for nuclear fragmentation, n=3. **(B)** Wt or Tg BMDM were challenged with
22 serotype 2 *S. pneumoniae* D39 (Spn) at a multiplicity of infection (MOI) of 10 in the
23 presence of LIPO-PBS or LIPO-CLOD. 4 h post-challenge numbers of intracellular
24 bacterial colony forming units (CFU) were assessed, n=3. **(C-D)** Non-Tg or Tg mice were
25 infected with serotype 1 *S. pneumoniae* (Spn) in the presence of LIPO-PBS or LIPO-
26 CLOD. Alveolar macrophage (AM) numbers in bronchoalveolar lavage (BAL) (C), and

1 AM apoptosis in BAL (D) were measured by microscopy 24 h post-challenge, both n=4,
2 *= p<0.05, 2-way ANOVA. (E-G) Non-Tg and Tg mice were challenged with 10⁵
3 serotype 1 Spn and liposome-encapsulated PBS (LIPO-PBS) or clodronate (LIPO-
4 CLOD). 24 h after challenge, CFU in the lung (E) and blood (F), and total
5 polymorphonuclear leukocyte (PMN) numbers in the BAL (G) were measured, n= 6-13
6 mice per group from 3 independent experiments. (H-I) Tg or non-Tg were instilled
7 intranasally with 10⁵ colony forming units of serotype 2 *S. pneumoniae* then immediately
8 treated with ABT-263 or sabutoclax. 24 h after challenge, CFU in the lung (H) and blood
9 (I) were measured (median + interquartile range), n= 8-10, *= p<0.05, unpaired Students
10 t-test, or 2-way ANOVA, for analyses within or between groups respectively. See also
11 Figure E9-10.

12

13 **Figure 6: *Staphylococcus aureus* infection does not trigger apoptosis-associated**
14 **killing.**

15 (A) Bone marrow-derived macrophages (BMDM) from CD68.hMcl-1 non-transgenic
16 (non-Tg) or transgenic (Tg) mice were challenged with *S. aureus* (Sa) at a multiplicity of
17 infection (MOI) of 5. BMDM were lysed at varying time points during a ‘pulse-chase’
18 to allow detection of intracellular bacterial colony forming units (CFU), n=3. (B) BMDM
19 apoptosis, in the same experiments, n=3. (C) BMDM were lysed for initial assessment
20 of CFU or incubated in lysostaphin for 2 h, before CFU estimation to assess bacterial
21 killing between the indicated time-points, n=3. (D) BMDM were challenged with Sa at
22 MOI of 5 for varying time periods, extracellular bacteria killed and BMDM incubated
23 with kanamycin and kanamycin resistant Sa, before extracellular bacteria were killed
24 with lysostaphin and intracellular CFU measured at the designated time-points. The
25 graph shows intracellular CFU, cultured in the presence of kanamycin to measure
26 kanamycin resistant (recently ingested) bacteria over each time increment, n=3. (E-G)

1 Non-Tg or Tg mice were challenged with Sa at the designated dose. 24 h post-challenge,
2 bacterial CFU in the lung homogenate (E), PMN numbers in the bronchoalveolar lavage
3 (BAL) (F) and alveolar macrophage (AM) apoptosis (G), were measured, n=4-9 mice per
4 group, from three independent experiments. See also Figure E11.

1 **Alveolar macrophage apoptosis-associated bacterial killing helps prevent murine**
2 **pneumonia.**

3

4 Julie A. Preston, Martin A. Bewley, Helen M. Marriott, A. McGarry Houghton,
5 Mohammed Mohasin, Jamil Jubrail, Lucy Morris, Yvonne L. Stephenson, Simon
6 Cross, David R. Greaves, Ruth W. Craig, Nicovan Rooijen, Colin D. Bingle, Robert
7 C. Read , Timothy J. Mitchell, Moira K.B. Whyte, Steven D. Shapiro and David H.
8 Dockrell

9

10

11

On Line Supplement

1 **Supplemental Methods.**

2 **Bacteria**

3 Serotype 2 *S. pneumoniae* (D39 strain, NCTC 7466) was grown as previously
4 described(1). Serotype 1 *S. pneumoniae* (WHO reference laboratory strain SSISP 1/1:
5 Statens Seruminstitut) was also grown as previously described and was used for *in vivo*
6 infection(2). A streptomycin resistant derivative of D39 (FP58) (3) was obtained from
7 Prof. Timothy Mitchell University of Birmingham. For experiments on human cells, *S.*
8 *pneumoniae* strains were opsonized in RPMI (Sigma-Aldrich) containing 10% human
9 anti-pneumococcal immune serum as previously described (1) or for murine cells with
10 murine serum containing detectable anti-pneumococcal antibodies (4). *Haemophilus*
11 *influenzae* type b Egan strain (H636) was obtained from Dr Derek Hood, University
12 of Oxford. *Staphylococcus aureus* Newman strain and a kanamycin resistant Newman
13 strain were obtained from Prof. Simon Foster, University of Sheffield. All infections
14 were carried out at a multiplicity of infection (MOI) of 10, to ensure a level of
15 intracellular bacteria that triggered apoptosis and overwhelmed initial phagolysosomal
16 killing mechanisms, except with *S. aureus* where lower MOI were used due to higher
17 levels of initial ingestion. After challenge, extracellular bacteria were washed off after
18 4 h, and media replaced.

19

20 **Isolation and culture of macrophages and other leukocytes**

21 Bone marrow-derived macrophages (BMDM) were obtained by culturing marrow for
22 14 days as previously described (2). Differentiation was confirmed by expression of
23 F4/80. Resident alveolar macrophages (AM) were collected by bronchoalveolar lavage
24 (BAL) with 4 aliquots of 0.8ml PBS. Peritoneal macrophages (PM) were collected 4
25 days after i.p. injection of 4% thioglycollate (5). AM and PM were enriched by 4 h

1 plastic adherence in RPMI (Lonza) + 10% FCS with low LPS. Murine neutrophils were
2 isolated from peripheral blood using negative immunomagnetic selection as previously
3 described (6), while murine CD19⁺ B-lymphocytes and CD3⁺ T-lymphocytes were
4 isolated using a fluorescent cell sorter (FACS Aria, BD Biosciences). Human
5 monocyte-derived macrophages (MDM) were isolated from whole blood donated by
6 healthy volunteers as previously described (1). In some experiments apoptosis was
7 induced *in vitro* by UV irradiation (120mJ/cm², Stratalinker 1800, Stratagene). As
8 indicated macrophages were incubated with 50 μ M 1400W (Calbiochem), an inhibitor
9 of iNOS, 50 μ M Trolox (Calbiochem), an antioxidant, or 1 mM Mito-TEMPO (Enzo),
10 an inhibitor of mitochondrial ROS or 50 μ M zVADfmk (Enzymes Systems Products),
11 an inhibitor of caspases or 50 μ M zFAfmk (Enzyme Systems Products) as zVADfmk's
12 control from 1 h prior to bacterial challenge and for the duration of bacterial exposure.

13

14 ***In vivo* infection**

15 Mcl-1 transgenic mice and non-transgenic littermates, from the same cages, were
16 inoculated with bacteria and tissues collected to determine viable bacteria, neutrophils
17 in lavage cytopins and apoptotic macrophages in lavage cytopins or by analysis of
18 flow cytometry as previously described (2).

19

20 **Bone marrow transfer**

21 Recipient mice were 6 week old C57BL/6J female mice (Charles River), maintained on
22 acidified water in individual ventilated cages and irradiated with 2 doses of 550 rads
23 separated by 4 h. Donor bone marrow, was obtained from CD68.hMcl-1⁺ transgenic
24 mice, or CD68.hMcl-1⁻ non-transgenic littermates, that had been backcrossed for 10
25 generations onto a C57BL/6J background. Bone marrow was isolated as described

previously (7) and resuspended in HBSS at approximately 1×10^7 cells/ml. 4 h after the second dose of radiation, 200 μ l of the bone marrow cell suspension was injected into each recipient mouse via the tail vein. The mice were maintained in individual ventilated cages with free access to autoclaved food and acidified water for 3 months before intratracheal instillation with 1×10^4 colony forming units of type 1 *S. pneumoniae* as described. We have previously documented that at this time point post-transplantation this protocol allows replacement of recipient alveolar macrophages with donor macrophages (8). We and others have also shown that the function of alveolar macrophages is reduced by the transplantation procedure and mice are more susceptible to infection with a given dose after transplantation and less able to effectively clear all bacteria when challenged with an inoculum mice that have not undergone an adoptive transplant procedure would have cleared (8, 9). Following adoptive bone marrow transfer, macrophage-associated bacteria were assessed by cytospin.

Neutrophil Depletion

Mcl-1 transgenic mice and non-transgenic littermates were injected i.p. with 200 μ g Ly6G specific antibody (eBioscience, functional grade, clone 1A8) to deplete circulating neutrophils 24h before intratracheal inoculation with 10^4 colony forming units of type 1 pneumococci.

Flow Cytometry

To detect murine cell surface markers, cells were incubated with 1 μ g ml⁻¹ F4/80-FITC (rat monoclonal IgG2b, clone CI:A3-1, AbD Serotec), CD19-PE (rat monoclonal, IgG2aK clone 1D3, BD Pharmingen), CD3-PE (rat monoclonal, IgG2bK clone 17A2, BD Pharmingen). In other experiments, cells were incubated with either 10 μ M 5,5',6,6'-tetrachloro-1,1',3,3'-tetraethylbenzimidazolylcarbocyanine iodide (JC-1;

1 Molecular Probes) to measure loss of inner mitochondrial transmembrane potential
2 ($\Delta\psi_m$) (8), RPMI containing 5 μ M acridine orange (Sigma-Aldrich) to measure loss
3 of lysosomal acidification (LLA) (8). Cells were incubated in phenol-red free RPMI
4 containing 5 μ M difluorescein diacetate (DAF-FM) (Sigma) to measure NO (10).
5 Caspase activity in live cells was analyzed using the CellEvent caspase 3/7 green flow
6 kit (Life Technologies). ROS were measured using 2', 7'-dichloro-dihydrofluorescein
7 diacetate (DCFDA; Sigma-Aldrich) (11) and mROS with MitoSOX-red (Invitrogen)
8 (12). Flow cytometric measurements were performed using a four colour
9 FACSCalibur (Becton Dickinson). Cell sorting was performed on a FACS Aria
10 (Becton Dickinson). Samples were resuspended in 200 μ L PBS, and forward and side
11 scatter light was used to identify cell populations and at least 10,000 events recorded
12 All data was analysed using FlowJo software, version 8.8.4 (Tree Star Inc.).

13

14 **Confocal microscopy.**

15 *Streptococcus pneumoniae* (D39) were labelled with Alexa Fluor-647 tagged
16 carboxylic acid succinimidyl ester as described previously (12, 13). Briefly, frozen
17 aliquots of bacteria were thawed out and resuspended in PBS at a cell density of 100
18 million colonies forming units per mL. A 500 μ L aliquot was removed, and 18.8 μ L of
19 0.5 mg/mL Alexa Fluor-647 carboxylic acid succinimidyl ester (Life Technologies) in
20 DMSO (Sigma Aldrich) was added and incubated in the dark for 1 h at room
21 temperature. The suspension was then centrifuged at 2000g for 10 min, the supernatant
22 was discarded, and the cell pellet was resuspended in 500 μ L of PBS and opsonized
23 with 10% mouse immunized pool serum for 30 min at 37°C. Macrophages were
24 challenged with labelled or vehicle treated bacteria as described (2), and at 16 h post-
25 challenge were stained with 10 μ M DAF-FM diacetate (Molecular probes, D23842) in

1 serum and phenol red free RPMI media for 30 min at 37°C and then 2.5 µM MitoSOX-
 2 red (Invitrogen) to detect mROS for 25 min at 37°C. To perform co-staining with
 3 phagolysosomes and ER after 16 h of bacterial challenge, macrophages were stained with
 4 or without DAF-FM, followed by MitoSOX-red , and then 1.0 µM cresyl violet acetate
 5 (Sigma, C10510540) for 20 min to detect lysosomes/phagolysosomes (2, 14) or 1.0 mM
 6 ER tracker red (Bodipy TR Glibenclamide, Life Technologies, E34250) for 20 min at
 7 37°C. Cells were then washed in HBSS three times, before being fixed in 2%
 8 paraformaldehyde. Cells were visualised using a 488 nm excitation and 500-530 nm
 9 emission detector for DAF-FM diacetate, 543 nm excitation and 565-615 nm emission
 10 detector for MitoSOX-red, 633 nm excitation, 640-704.2 nm emission for Alexa Fluor-
 11 647 carboxylic acid succinimidyl ester and cresyl violet, 543 nm excitation and 560 nm
 12 emission detector for ER tracker red with a Axiovert 200M Zeiss LSM510 inverted
 13 confocal fluorescence microscope using a 63x1.4 NA oil objective lens. Representative
 14 confocal images (supplementary Figures E4-6) were created from the region of interests
 15 (ROI) of maximum projected z-sections images (Size scaling: 0.07x0.07x0.48µm,
 16 Scan zoom 2 and average line 4) using a 17x17 hat filter with intermodal black and
 17 white threshold correction by ImageJ, as described previously (15). The Pearson's
 18 correlation coefficient was calculated as described previously in (16). The corrected
 19 integrated total cell fluorescence intensity for NO and mROS were quantified using
 20 ImageJ (v1.48, NIH), as described previously by McCloy RA *et al.*, (17). Briefly, the
 21 individual channels for Z-sections images were separated and the maximum Z-
 22 projected images were generated by ImageJ (*e.g.* Image>Stack>Z projected).
 23 Subsequently, the corrected integrated total cell fluorescence was calculated using the
 24 following formula, the corrected total cell fluorescence (CTCF) = integrated density –
 25 (area of selected cell × mean fluorescence of background readings), as calculated from

1 the free-hand selected outline for each cell. Similarly, a ROI was selected from the
2 separated channel-1 or channel-2 images to quantify the correlation coefficient for NO
3 versus mROS or phagolysosome fluorescence and NO versus mROS or bacteria as
4 described (15). The digital distance between NO and mROS or bacteria or
5 phagolysosomes or between ER and NO or bacteria or phagolysosomes was measured
6 by ImageJ. From this analysis, the signals were classified as being in proximity if the
7 shortest distance between signals was ≤ 80 nm.

8

9 **Intracellular killing assay.**

10 Assessment of intracellular pneumococcal viability was carried out as previously
11 described (10). After the indicated time points macrophages were incubated in RPMI
12 containing $20\mu\text{g ml}^{-1}$ gentamicin (Sanofi) and $50\mu\text{U}$ penicillin (Sigma) for 30 min to
13 kill extracellular bacteria before being lysed with 2% saponin for 12 min. Lysates
14 were diluted to 1ml in PBS, and intracellular bacterial numbers determined by Miles-
15 Misra surface viable count. All killing assays were performed in duplicate wells.
16 Early bacterial recovery (≤ 4 h) is a function of both initial phagocytosis and early
17 intracellular killing but correlates well with assessment of phagocytosis by
18 microscopy based analysis and estimation of phagocytic index (1, 2, 18, 19). To
19 assess the kinetics of intracellular bacterial killing a 'pulse-chase' design was
20 performed in which extracellular bacteria were killed with gentamicin/penicillin and
21 then cultures were placed in RPMI containing vancomycin ($0.75\mu\text{g ml}^{-1}$; Sigma), to
22 ensure extracellular bacteria remained undetectable with an antimicrobial that lacked
23 significant intracellular penetration, before macrophage lysis at the indicated time
24 points as above (Fig. 4E). In experiments to assess killing over a fixed time interval,
25 internalization of bacteria was measured at the first time point, while duplicate wells

1 were incubated with vancomycin for a further 2 h before macrophage lysis. At all
2 time-points, surface viable counts were also performed on media supernatants to
3 confirm antibiotic killing of extracellular bacteria (Fig. 4H). In experiments to assess
4 the rate of ongoing bacterial internalization, cultures at the indicated time points were
5 incubated with 20 μ g ml⁻¹ gentamicin and 50 μ U penicillin for 30 min to kill
6 extracellular bacteria before being split into two sets. The first were incubated with
7 vancomycin and the kinetics of intracellular killing measured and the second set
8 received a second pulse with a streptomycin resistant derivative of D39, FP58, at an
9 MOI of 10, in the presence of 10 μ g ml⁻¹ streptomycin (Fig. 4I). Two hours after the
10 addition of this second pulse, extracellular bacteria were killed with penicillin and
11 gentamicin as above and cells were lysed using saponin as above. Lysates were plated
12 out on blood agar plates with or without streptomycin (10 μ g ml⁻¹), to ascertain the
13 number of intracellular bacteria originating from the second pulse over the preceding
14 2 h. Assays for intracellular killing of *S. aureus* were similar except that initial killing
15 of extracellular bacteria used lysostaphin at 20 μ g ml⁻¹ (instead of gentamicin and
16 penicillin) and used lysostaphin at 2 μ g ml⁻¹ to maintain undetectable extracellular
17 bacteria in a pulse-chase design to measure the kinetics of intracellular killing or the
18 killing over a fixed time interval (20). Surface viable counts confirmed killing of
19 extracellular bacteria with these approaches. To measure ongoing internalization
20 extracellular bacteria were killed with kanamycin at 50 μ g ml⁻¹ and then cells received
21 a second 'pulse' of bacteria with kanamycin resistant *S. aureus* (KanR) in the
22 presence of media containing 50 μ g ml⁻¹ kanamycin. Two hours after the second
23 'pulse', 20 μ g ml⁻¹ lysostaphin was added for 30 minutes to kill extracellular KanR
24 bacteria, the cells were lysed and lysates plated out in the presence or absence of 50 μ g
25 ml⁻¹ kanamycin (Fig. 2g).

1

2 **Reconstitution of Apoptosis**

3 Apoptosis was reconstituted *in vitro* with clodronate-encapsulated liposomes (5 mg ml⁻¹
4 clodronate) or 0.2 μ M ABT-737, 20 μ M AT101, 20 μ M UMI-77 or 20 μ M Sabutoclax
5 (all Selleck Chemicals). Clodronate was a gift of Roche Diagnostics GmbH,
6 Mannheim, Germany. *In vivo* apoptosis of AM was reconstituted in transgenic mice
7 using a modified clodronate-liposome protocol and clodronate containing liposomes
8 supplied by Dr Nico von Rooijen (UMC Amsterdam) (21). *In vivo* reconstitution of
9 apoptosis was achieved using the Bcl-2 specific agent ABT-263 (50mg kg⁻¹, ip), a
10 derivative of ABT-737, and sabutoclax (5mg kg⁻¹, ip), a pan-Bcl-2 inhibitor with
11 inhibitory activity against Mcl-1 (22-24). Doses of all compounds were selected as
12 doses that overcame intrinsic resistance to apoptosis and induced apoptosis in
13 transgenic cells at comparable levels to bacterial infection in non-transgenic cells in the
14 absence of compound.

15

16 **SDS-Page and western blot**

17 Whole cell extracts were isolated using SDS-lysis buffer as described before (10) and
18 equal protein loaded per lane. Proteins were separated by SDS gel electrophoresis,
19 blotted onto a PVDF membrane, and blocked for 60 min at room temperature in PBS
20 containing 0.05% Tween with 5% (v/w) skim milk powder. Membranes were incubated
21 overnight at 4°C with antibodies against human Mcl-1 (mouse monoclonal; 1:1000; BD
22 Pharmingen) (25), mouse Mcl-1 (rabbit polyclonal; 1:1000; Rockland), human/mouse
23 Mcl-1 (rabbit polyclonal SC-19; 1:1000; Santa Cruz), cytochrome *c* (mouse
24 monoclonal clone 7H82C12 IgG2b; 1:1000; BD Pharmingen), cathepsin B (mouse
25 monoclonal clone CA10 IgG2a; 1:1000; Abcam) or β -actin (rabbit polyclonal; 1:5000;

1 Sigma). Proteins were detected using HRP-conjugated secondary antibodies (1:2000;
2 Dako) and ECL (Amersham Pharmacia). Bands were quantified using Image J 1.32
3 software (NIH). Fold change from mock-infected was calculated and normalized to the
4 fold change in actin.

5

6 **Caspase activation**

7 Cellular caspase activity was measured using the Caspase-Glo 3/7 assay (Promega)
8 according to manufacturer's instructions. Luminescence was measured on a Varioskan
9 Flash multimode reader (Thermo Scientific).

10

11 **Cathepsin D Activation**

12 Cathepsin D activity was measured using a fluorometric cathepsin D activity assay kit
13 (Abcam) in accordance with the manufacturer's instructions (8). Fluorescence was
14 measured on a Varioskan Flash multimode reader (Thermo Scientific). Cathepsin D
15 activity in each sample was expressed as percentage of a comparative sample that had
16 been treated with 500 μ M pepstatin A to act as a negative control.

17

18 **Apoptosis**

19 Nuclear fragmentation and condensation indicative of apoptosis were detected using
20 4'6'-diamidino-2-phenylindole (DAPI) (1).

21

22 **Cytokine ELISA**

23 Cytokines in BMDM supernatants were measured with Ready-SET-Go ELISA
24 reagent sets (eBioscience, San Diego, CA) for mouse tumor necrosis factor (TNF),

IL-1 β and IL-6 in accordance with the manufacturer's protocols. Limits of detection were 8, 8 and 4 pg/ml respectively.

Histopathology of murine tissue

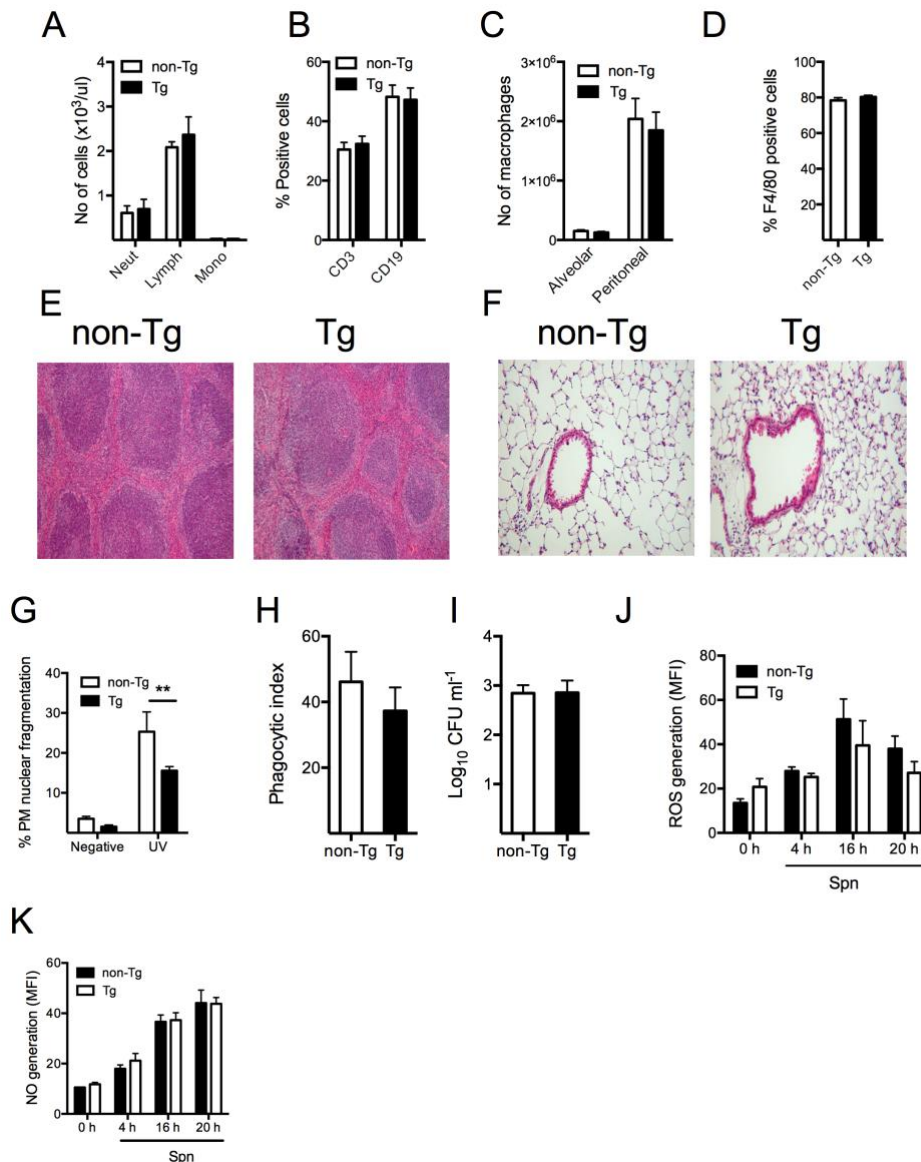
Histopathological analysis of tissue sections from mice for analysis of tissue architecture was performed by a pathologist (SC), blinded to the origin of samples, as previously described using Zeiss Axoplan 2E microscope (Zeiss, Oberkochen, Germany) (2). Spleen and lung were visualised with 10X and 20X objective respectively.

References

1. Dockrell DH, Lee M, Lynch DH, Read RC. Immune-mediated phagocytosis and killing of *Streptococcus pneumoniae* are associated with direct and bystander macrophage apoptosis. *J Infect Dis* 2001; 184: 713-722.
2. Dockrell DH, Marriott HM, Prince LR, Ridger VC, Ince PG, Hellewell PG, Whyte MK. Alveolar macrophage apoptosis contributes to pneumococcal clearance in a resolving model of pulmonary infection. *J Immunol* 2003; 171: 5380-5388.
3. Iannelli F, Chiavolini D, Ricci S, Oggioni MR, Pozzi G. Pneumococcal surface protein C contributes to sepsis caused by *Streptococcus pneumoniae* in mice. *Infect Immun* 2004; 72: 3077-3080.
4. Marriott HM, Bingle CD, Read RC, Braley KE, Kroemer G, Hellewell PG, Craig RW, Whyte MK, Dockrell DH. Dynamic changes in Mcl-1 expression regulate macrophage viability or commitment to apoptosis during bacterial clearance. *J Clin Invest* 2005; 115: 359-368.
5. Shipley JM, Wesselschmidt RL, Kobayashi DK, Ley TJ, Shapiro SD. Metalloelastase is required for macrophage-mediated proteolysis and matrix invasion in mice. *Proc Natl Acad Sci U S A* 1996; 93: 3942-3946.
6. Cotter MJ, Norman KE, Hellewell PG, Ridger VC. A novel method for isolation of neutrophils from murine blood using negative immunomagnetic separation. *Am J Pathol* 2001; 159: 473-481.
7. Tulone C, Uchiyama Y, Novelli M, Grosvenor N, Saftig P, Chain BM. Haematopoietic development and immunological function in the absence of cathepsin D. *BMC Immunol* 2007; 8: 22.
8. Bewley MA, Marriott HM, Tulone C, Francis SE, Mitchell TJ, Read RC, Chain B, Kroemer G, Whyte MK, Dockrell DH. A cardinal role for cathepsin d in co-ordinating the host-mediated apoptosis of macrophages and killing of pneumococci. *PLoS pathogens* 2011; 7: e1001262.
9. Ojielo CI, Cooke K, Mancuso P, Standiford TJ, Olkiewicz KM, Clouthier S, Corrion L, Ballinger MN, Toews GB, Paine R, 3rd, Moore BB. Defective

- phagocytosis and clearance of *Pseudomonas aeruginosa* in the lung following bone marrow transplantation. *J Immunol* 2003; 171: 4416-4424.
10. Marriott HM, Ali F, Read RC, Mitchell TJ, Whyte MK, Dockrell DH. Nitric oxide levels regulate macrophage commitment to apoptosis or necrosis during pneumococcal infection. *The FASEB journal : official publication of the Federation of American Societies for Experimental Biology* 2004; 18: 1126-1128.
11. Hiraoka W, Vazquez N, Nieves-Neira W, Chanock SJ, Pommier Y. Role of oxygen radicals generated by NADPH oxidase in apoptosis induced in human leukemia cells. *J Clin Invest* 1998; 102: 1961-1968.
12. Mukhopadhyay P, Rajesh M, Hasko G, Hawkins BJ, Madesh M, Pacher P. Simultaneous detection of apoptosis and mitochondrial superoxide production in live cells by flow cytometry and confocal microscopy. *Nat Protoc* 2007; 2: 2295-2301.
13. Gunsolus IL, Hu D, Mihai C, Lohse SE, Lee CS, Torelli MD, Hamers RJ, Murhpy CJ, Orr G, Haynes CL. Facile method to stain the bacterial cell surface for super-resolution fluorescence microscopy. *Analyst* 2014; 139: 3174-3178.
14. Ostrowski PP, Fairn GD, Grinstein S, Johnson DE. Cresyl violet: a superior fluorescent lysosomal marker. *Traffic* 2016; 17: 1313-1321.
15. Bewley MA, Preston JA, Mohasin M, Marriott HM, Budd RC, Swales J, Collini P, Greaves DR, Craig RW, Brightling CE, Donnelly LE, Barnes PJ, Singh D, Shapiro SD, Whyte MKB, Dockrell DH. Impaired Mitochondrial Microbicidal Responses in Chronic Obstructive Pulmonary Disease Macrophages. *Am J Respir Crit Care Med* 2017; 196: 845-855.
16. Dunn KW, Kamocka MM, McDonald JH. A practical guide to evaluating colocalization in biological microscopy. *Am J Physiol Cell Physiol* 2011; 300: C723-742.
17. McCloy RA, Rogers S, Caldon CE, Lorca T, Castro A, Burgess A. Partial inhibition of Cdk1 in G 2 phase overrides the SAC and decouples mitotic events. *Cell Cycle* 2014; 13: 1400-1412.
18. Gordon SB, Irving GR, Lawson RA, Lee ME, Read RC. Intracellular trafficking and killing of *Streptococcus pneumoniae* by human alveolar macrophages are influenced by opsonins. *Infect Immun* 2000; 68: 2286-2293.
19. Jubrail J, Morris P, Bewley MA, Stoneham S, Johnston SA, Foster SJ, Peden AA, Read RC, Marriott HM, Dockrell DH. Inability to sustain intraphagolysosomal killing of *Staphylococcus aureus* predisposes to bacterial persistence in macrophages. *Cellular microbiology* 2016; 18: 80-96.
20. Schuhardt VT, Schindler CA. Lysostaphin Therapy in Mice Infected with *Staphylococcus Aureus*. *J Bacteriol* 1964; 88: 815-816.
21. Van Rooijen N, Sanders A. Liposome mediated depletion of macrophages: mechanism of action, preparation of liposomes and applications. *J Immunol Methods* 1994; 174: 83-93.
22. Bajwa N, Liao C, Nikolovska-Coleska Z. Inhibitors of the anti-apoptotic Bcl-2 proteins: a patent review. *Expert Opin Ther Pat* 2012; 22: 37-55.
23. Dash R, Azab B, Quinn BA, Shen X, Wang XY, Das SK, Rahmani M, Wei J, Hedvat M, Dent P, Dmitriev IP, Curiel DT, Grant S, Wu B, Stebbins JL, Pellecchia M, Reed JC, Sarkar D, Fisher PB. Apogossypol derivative BI-97C1 (Sabutoclax) targeting Mcl-1 sensitizes prostate cancer cells to mda-7/IL-24-mediated toxicity. *Proc Natl Acad Sci U S A* 2011; 108: 8785-8790.

- 1 24. Speir M, Lawlor KE, Glaser SP, Abraham G, Chow S, Vogrin A, Schulze KE,
2 Schuelein R, O'Reilly LA, Mason K, Hartland EL, Lithgow T, Strasser A,
3 Lessene G, Huang DC, Vince JE, Naderer T. Eliminating Legionella by
4 inhibiting BCL-XL to induce macrophage apoptosis. *Nat Microbiol* 2016; 1:
5 15034.
6 25. Yang T, Kozopas KM, Craig RW. The intracellular distribution and pattern of
7 expression of Mcl-1 overlap with, but are not identical to, those of Bcl-2. *The*
8 *Journal of cell biology* 1995; 128: 1173-1184.
9



10
11 **Figure E1: hMcl-1 transgenic mice lack gross immunological or pulmonary**
12 **phenotypes and have unaltered early immune responses.**
13 (A) Peripheral blood was taken from naïve (unchallenged) CD68.hMcl-1 non-
14 transgenic (non-Tg) or transgenic (Tg) mice, and total cell counts were performed for
15 neutrophils (Neut), lymphocytes (Lymph) and monocytes (Mono), n=4. (B) Spleen
16 cells from non-Tg or Tg mice were harvested and the percentage of CD3⁺ T-

1 lymphocytes (CD3) and CD19⁺ B-lymphocytes (CD19) assessed by flow cytometry,
2 n=7. **(C)** The total number of macrophages in alveolar and peritoneal lavage of naïve
3 non-Tg and Tg mice, n=9. **(D)** BMDM from non-Tg or Tg mice were differentiated for
4 14 d and the percentage of macrophages positive for surface expression of the murine
5 macrophage marker F4/80 was assessed by flow cytometry, n=4. **(E-F)** Hematoxylin
6 and eosin stained spleens (E) and lungs (F) from non-Tg or Tg mice were reviewed
7 histopathologically. Tg spleens and lungs displayed normal features. Images are
8 representative of three organs analyzed per group. **(G)** Peritoneal (PM) macrophages
9 from non-Tg or Tg mice were left untreated (negative), or UV treated. 8 h after UV
10 exposure, apoptosis was assessed by nuclear fragmentation, n=6, **= p<0.01, ***=
11 p<0.001 2-way ANOVA. **(H-I)** BMDM from non-Tg or Tg mice were challenged with
12 latex beads (H) or serotype 2 *S. pneumoniae* (Spn) (I). Four hours post-challenge,
13 internalization of beads was analyzed by microscopy, n=9, or viable intracellular
14 colony forming units (CFU) were determined, n=5. **(J-K)** BMDM from non-Tg or Tg
15 mice were challenged with serotype 2 *S. pneumoniae* (Spn). At the designated time
16 post-challenge, production of reactive oxygen species (ROS) (J) and nitric oxide (NO)
17 (K) was measured by flow cytometry and median fluorescence intensity (MFI)
18 recorded. For both experiments, n=3. In all experiments, there were no significant
19 differences between groups.

20

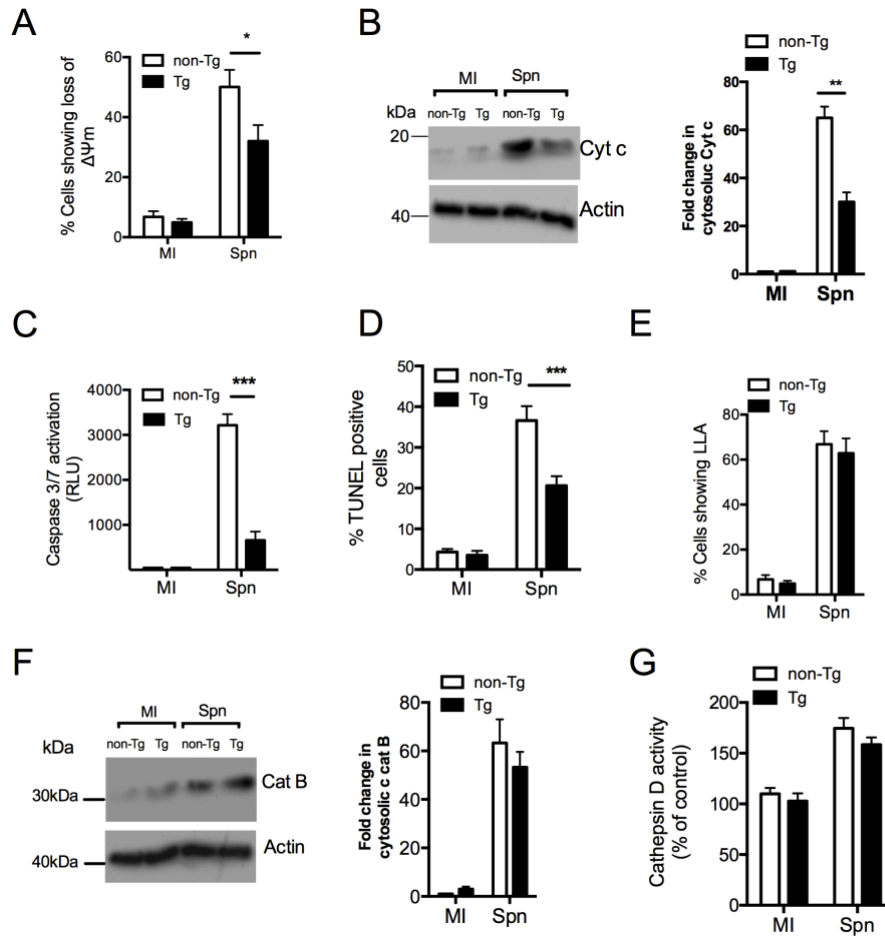


Figure E2: Mcl-1 modifies the mitochondrial pathway of apoptosis but not upstream phagolysosomal events in macrophages following bacterial challenge.

Bone marrow-derived macrophages (BMDM) from CD68.hMcl-1 non-transgenic (non-Tg) or CD68.hMcl-1 transgenic (Tg) mice were mock-infected (MI) or challenged with serotype 2 *S. pneumoniae* (Spn). (A-D) 16 h post-challenge cells were assessed to determine either (A) the percentage of cells with loss of mitochondrial inner transmembrane potential ($\Delta\psi_m$) by flow cytometry, n=4, (B) were fractionated into membrane and cytosolic fractions and the cytosolic fraction probed for cytochrome c, as a marker of mitochondrial outer membrane permeabilization, (C) were assessed for caspase 3/7 activation measuring relative luminescence units (RLU), n=9, or (D) were assessed for DNA cleavage at 20 h by TUNEL staining, n=4. (E-F) 16 h post-challenge cells were assessed to determine (E) the percentage of cells with loss of lysosomal acidification (LLA) by flow cytometry, n=4 or (F) fractionated and cytosolic fractions probed for cathepsin B, as a marker of lysosomal membrane permeabilization, by western blot. (G) 8 h post-challenge cells were assessed for cathepsin D activity, n=4. For all experiments, * = $p < 0.05$ *** = $p < 0.001$, 2-way ANOVA. Blots are representative of four independent experiments

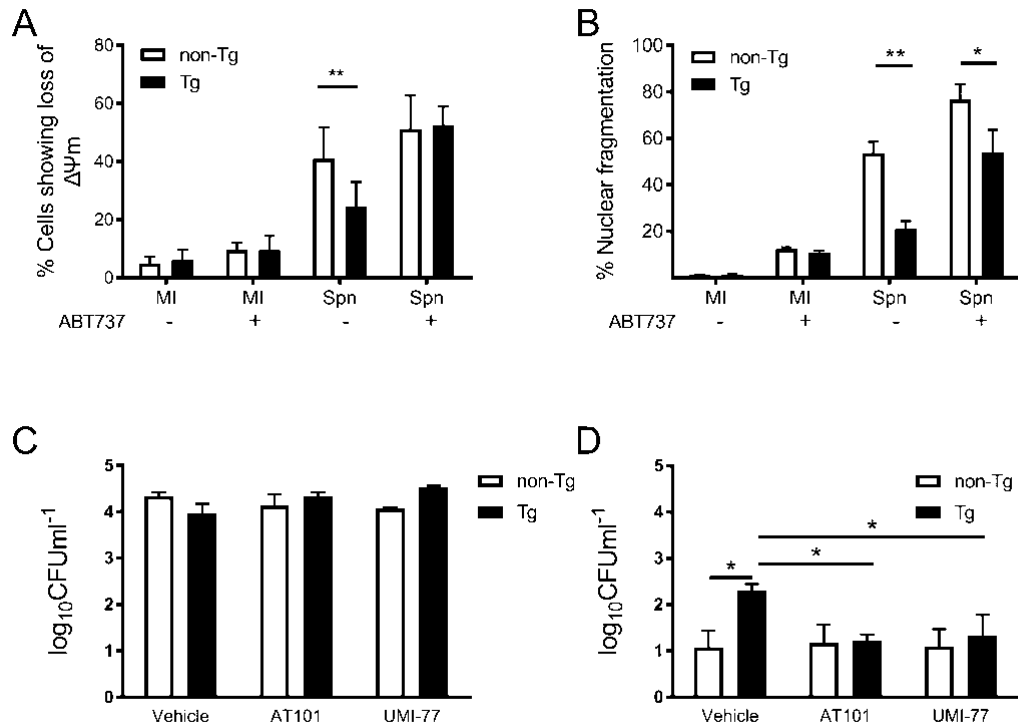


Figure E3: BH3 mimetics reconstitute apoptosis-associated killing.

(A-B) Bone marrow-derived macrophages (BMDM) from CD68.hMcl-1 non-transgenic (non-Tg) or CD68.hMcl-1 transgenic (Tg) mice were mock-infected (MI) or challenged with serotype 2 *S. pneumoniae* (Spn) in the presence (+) or absence (-) of ABT737. (A) 16 h post-challenge cells were assessed for loss of inner mitochondrial transmembrane potential ($\Delta\psi_m$) by flow cytometry and the percentage of cells with loss of $\Delta\psi_m$ recorded, n=6. (B) At 20 h post-challenge cells were assessed for apoptosis, as assessed by nuclear fragmentation, n=6. (C-D) BMDM were infected with serotype 2 *S. pneumoniae* after treatment with BH3 mimetics AT101 or UMI-77 or vehicle control and number of viable intracellular bacteria assessed at (C) 4h, n=3 or (D) 20h, n=4. In all experiments *= p<0.05, **= p<0.01; 2-way ANOVA.

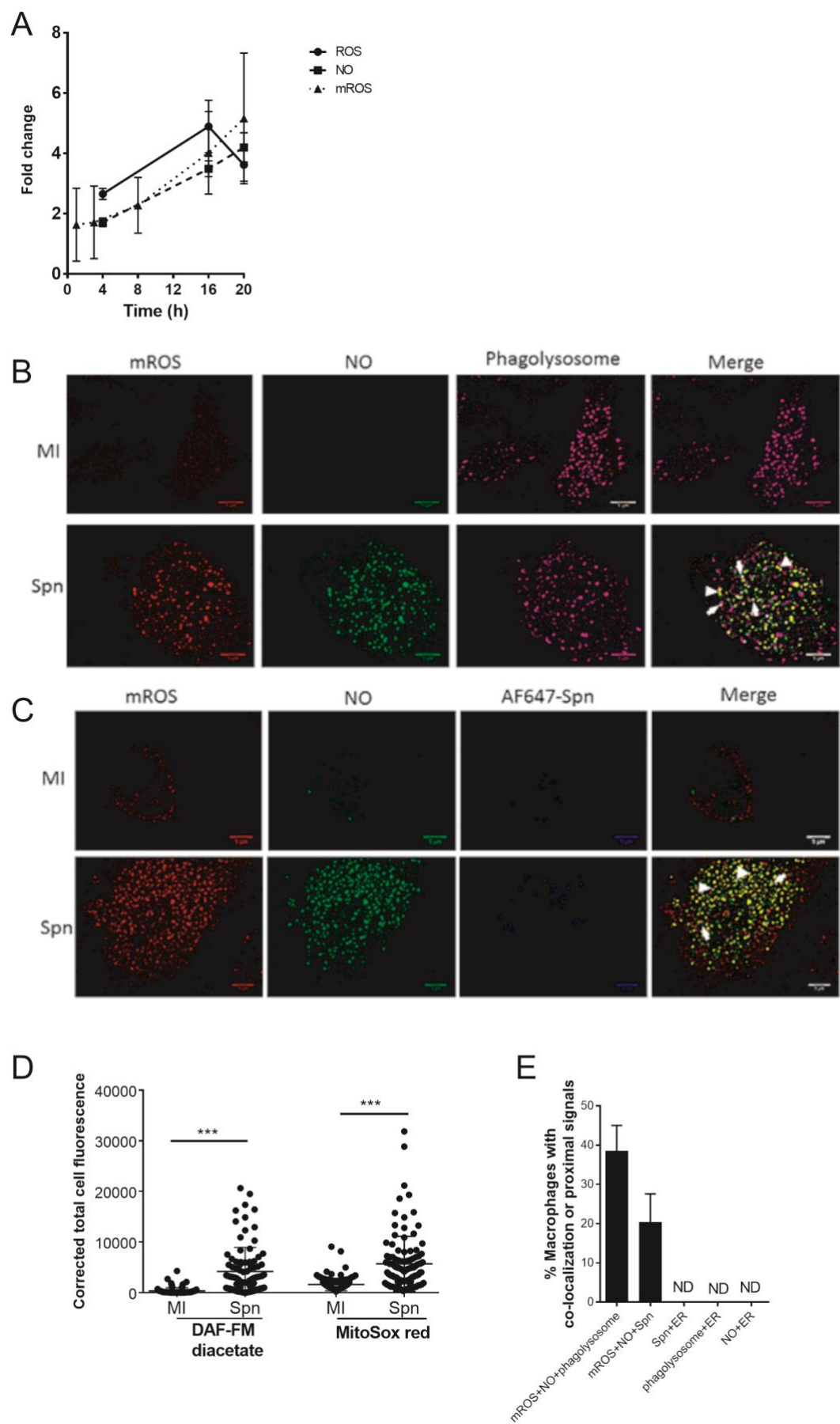


Figure E4: Macrophages mitochondrial ROS and NO colocalize with *S. pneumoniae* in the phagolysosomal compartment.

(A) Bone marrow-derived macrophages (BMDM) from CD68.hMcl-1 non-transgenic mice were challenged with serotype 2 *S. pneumoniae* (Spn). At the designated times post challenge production of reactive oxygen species (ROS), nitric oxide (NO) and mitochondrial reactive oxygen species (mROS) were measured by flow cytometry, n=3. (B-E) BMDM were exposed to unlabelled or Alexa Fluor-647 conjugated succinimidyl ester labelled opsonized Spn (AF647-Spn) for 16 h. mROS was stained with MitoSOX-red and NO stained with 4-Amino-5-Methylamino-2',7'-Difluorofluorescein (DAF-FM) diacetate and phagolysosomes with cresyl violet acetate. Figure (B) shows the representative fluorescence images for mROS (red), NO (green) and phagolysosomes (pink) in mock-infected (MI) BMDM (upper panel) and BMDM challenged with unlabelled Spn (lower panel). The co-localization signals between mROS and NO (yellow pixels) are labelled by the triangular arrows and the co-localization signals with phagolysosomes (white pixels) are labelled by the closed head arrows. Figure (C) shows the representative fluorescence images of mROS (red), NO (green) and AF647- Spn (blue) in MI (upper panel) and AF647-Spn exposed BMDM (lower panel). The co-localization signals between mROS, NO and intracellular AF647- Spn (yellow pixels) are shown by the triangular arrows and proximal signals are labelled by the closed head arrows in the merged image. Scale bars = 5 μ m. Figure (D) shows the corrected total cell fluorescence intensity (CTCF) for DAF-FM diacetate and MitoSOX red staining in MI and Spn exposed BMDM from these experiments. Figure (E) shows the percentages of macrophages which show either co-localization signals or proximal signals for the indicated combinations, which also include samples stained to identify endoplasmic reticulum (ER) with ER-Tracker Red. The CTCF and co-localization or proximal signals were measured from three independent experiments. ND = none detected. Data are shown as mean \pm SD and statistical analysis was performed with One-way ANOVA and Sidak's multiple comparison post-hoc test. ***p<0.001, n=3.

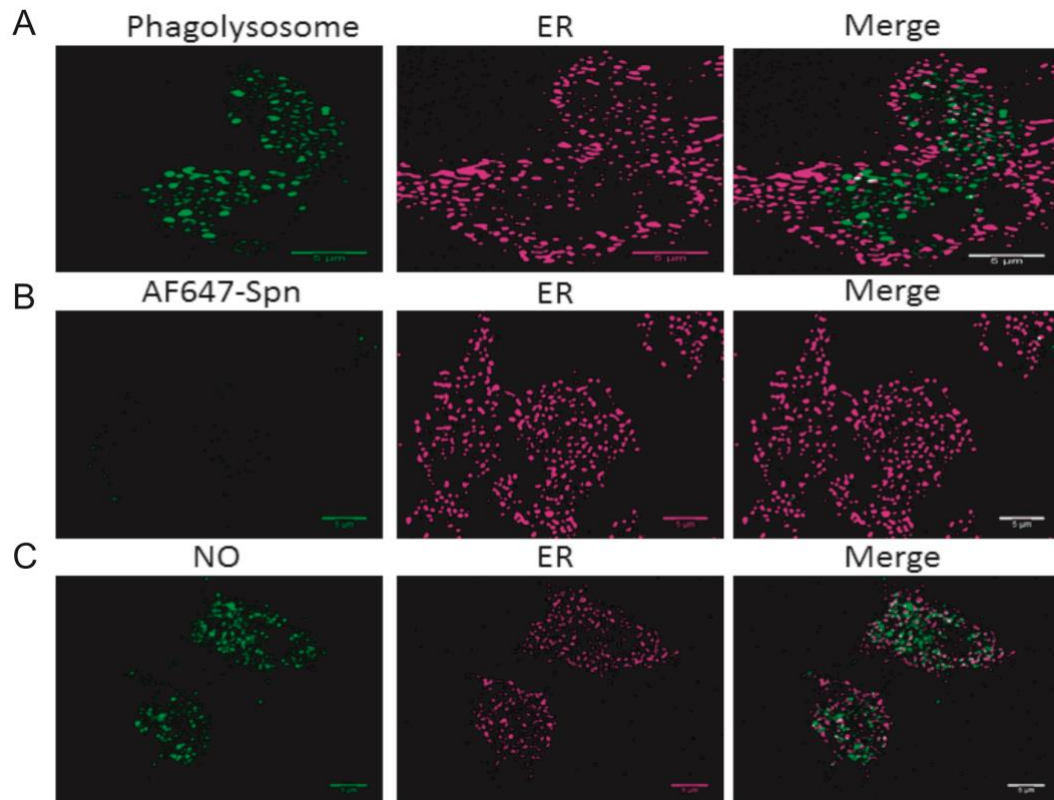


Figure E5: Phagolysosomes, Spn and NO do not co-localise with ER. Mouse bone marrow derived macrophages (BMDM) were challenged with Alexa Fluor-647 conjugated succinimidyl ester labelled opsonized *S. pneumoniae* (AF-647 Spn) for 16 hours followed by co-staining with ER-Tracker Red and cresyl violet to stain phagolysosomes or 4-Amino-5-Methylamino-2', 7'-Difluorofluorescein (DAF-FM) diacetate to stain NO. Representative confocal images show no co-localization of ER and phagolysosomes (panel A), ER and AF647-Spn (panel B) or ER and NO (panel C). Scale bars = 5 μm. The images are representative of three independent experiments.

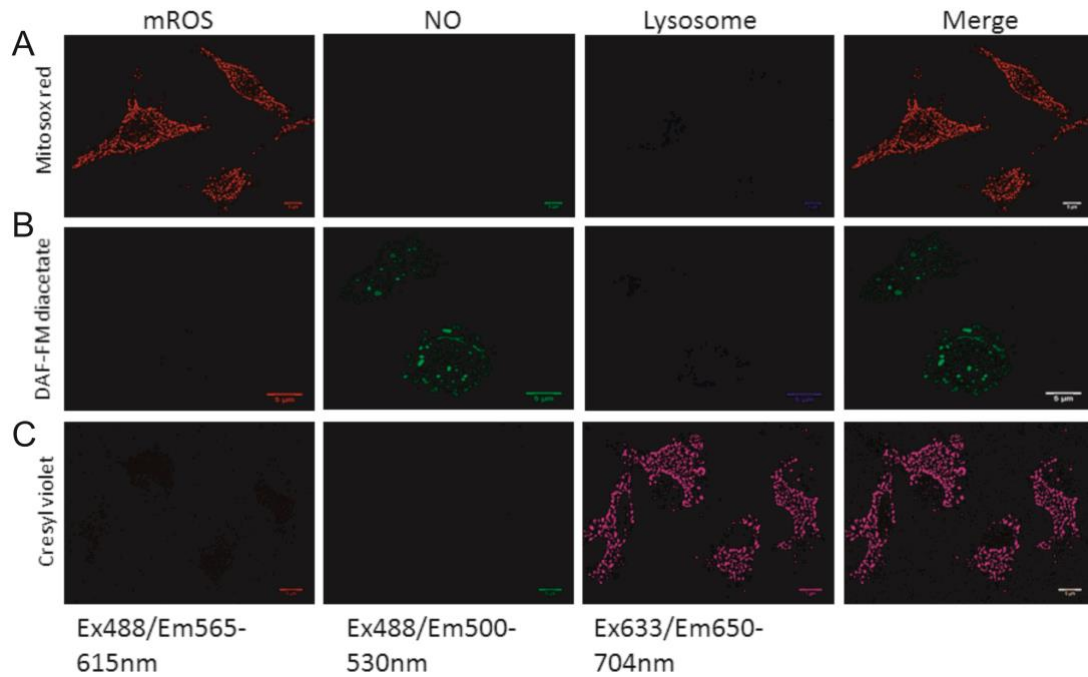
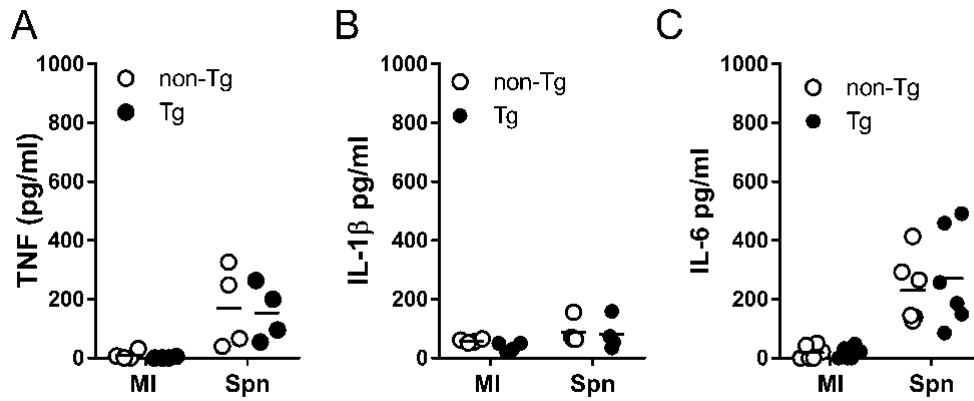


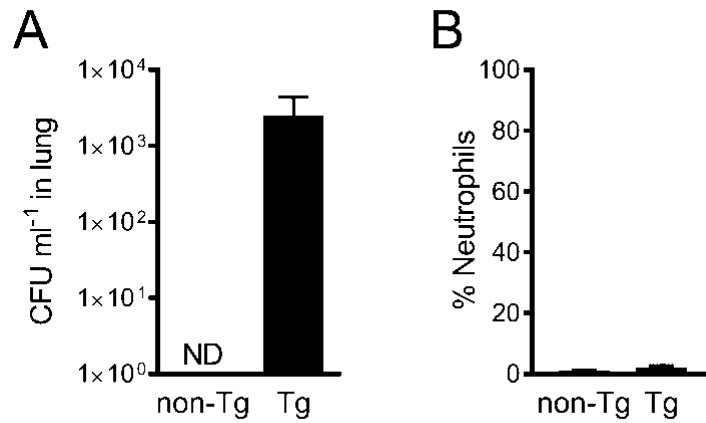
Figure E6: Phagolysosomal staining does not influence detection of nitric oxide or mROS. Mouse bone marrow derived macrophages (BMDM) were challenged with *S. pneumoniae* for 16 hours followed by single staining with either MitoSOX red to detect mROS (A), 4-Amino-5-Methylamino-2', 7'-Difluorofluorescein (DAF-FM) diacetate to detect NO (B) or with cresyl violet to stain lysosomes/phagolysosomes (C). Images show no significant background in the unstained channels after each stain individually. Scale bars = 5 μ m. Images are representative of three independent experiments.



1

2 **Figure E7: Cytokine production is not altered in hMcl-1 transgenic**
3 **macrophages**

4 (A-C) Bone marrow-derived macrophages (BMDM) from CD68.hMcl-1 non-
5 transgenic (non-Tg) or CD68.hMcl-1 transgenic (Tg) mice were challenged with
6 serotype 2 *S. pneumoniae* (Spn). 16 h post-challenge production of TNF (A), IL-1 β
7 (B), or IL-6 (C) was measured, n=4-6.



1

2 **Figure E8: Neutrophil depletion**

3 CD68.hMcl-1 transgenic (Tg) mice or CD68.hMcl-1 non-transgenic littermates (non-
4 Tg) were treated with Ly6G antibody to deplete circulating neutrophils 24h before
5 intratracheal infection with 10^4 colony forming units of serotype 1 *S. pneumoniae*. 24
6 h post infection the total colony forming units (CFU) in lung (A) were measured and
7 percentage of neutrophils (B) in in bronchoalveolar lavage (BAL) were calculated by
8 analysis of cytopins. ND = none detected, n = 7 per group.

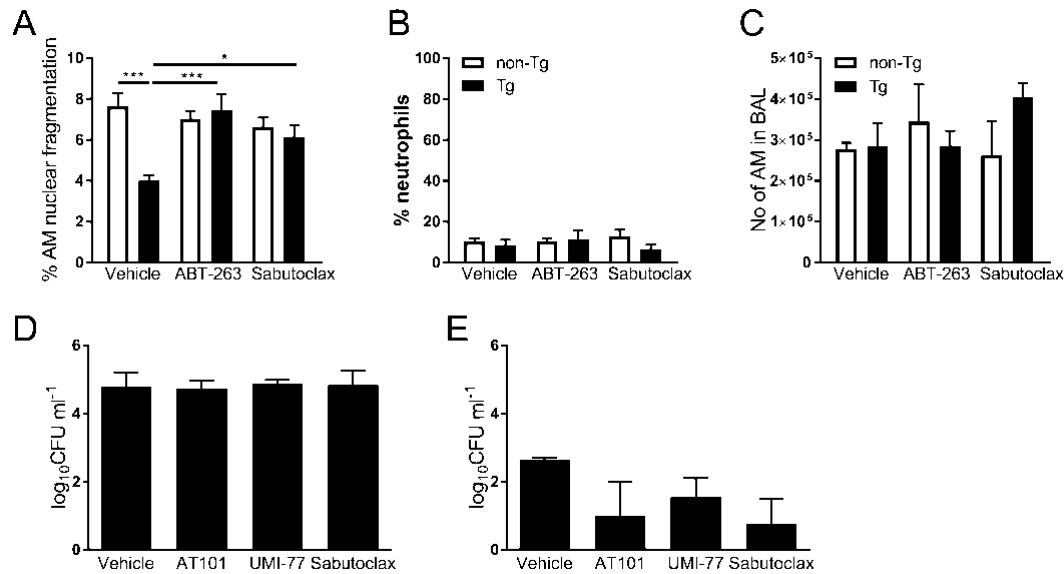
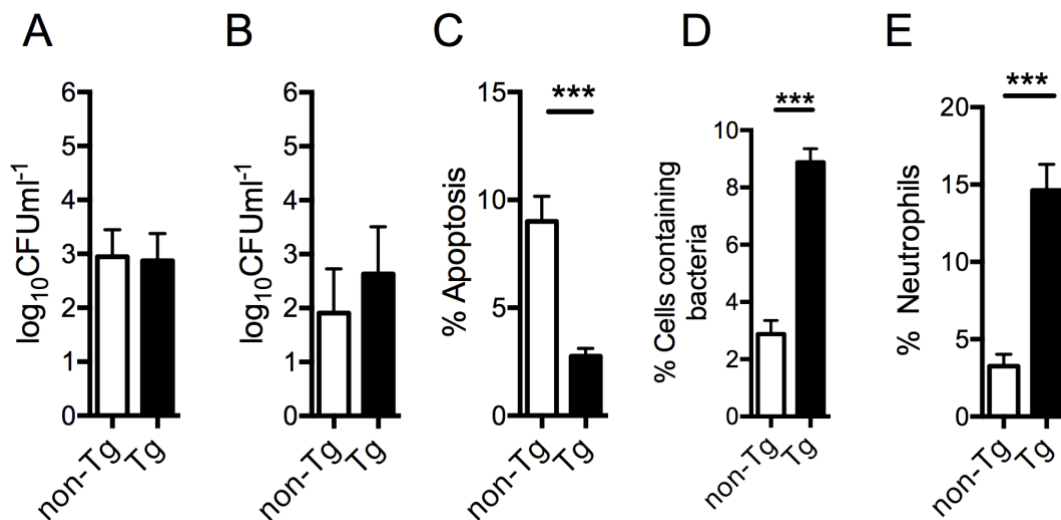


Figure E9: Reconstitution of apoptosis

(A-C) CD68.hMcl-1 transgenic (Tg) mice or CD68.hMcl-1 non-transgenic littermates (non-Tg) were instilled intranasally with 10⁵ colony forming units of serotype 2 *S. pneumoniae* then immediately treated with ABT-263 or salbutoclast. 24 h post infection the percentage of apoptotic cells (A), percentage of neutrophils (B) and number of alveolar macrophages (AM) in bronchoalveolar lavage (BAL) were calculated by analysis of cytopins, n = 10 per group. (D-E) Human monocyte derived macrophages were challenged with serotype 2 *S. pneumoniae* (Spn) at a multiplicity of infection (MOI) of 10 for 4h (D) or 16 h (E) in the presence of AT101, UMI-77, salbutoclast or vehicle control, n=3, vehicle vs. salbutoclast p=0.05. *** = p<0.001, * = p<0.05 2-way ANOVA with Sidak's multiple comparisons test or One-way ANOVA (D-E only).

1



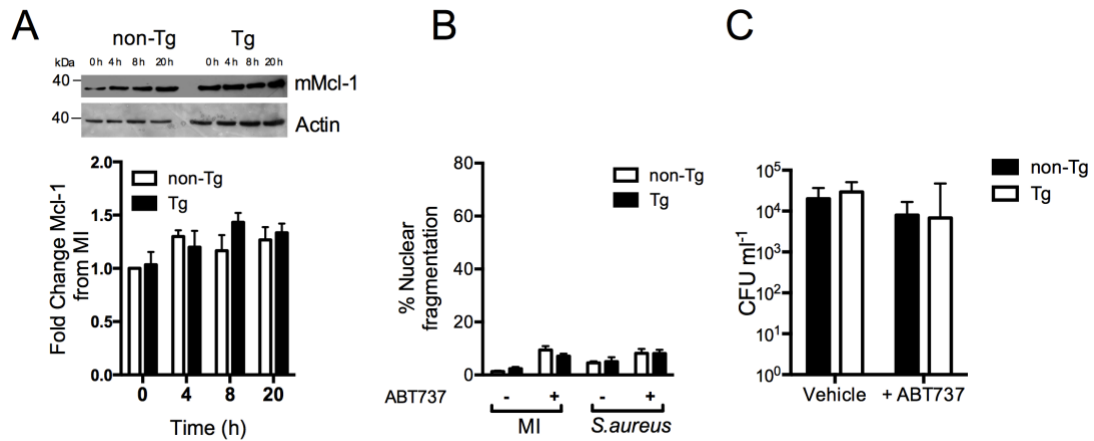
2

Figure E10: Adoptive bone marrow transplant

Mice were transplanted with bone marrow from CD68.hMcl-1 transgenic (Tg) mice or CD68.hMcl-1 non-transgenic littermates (non-Tg). Mice were instilled with 10^4 colony forming units of serotype 1 *S. pneumoniae* for 24 h before the total colony forming units (CFU) in lung (A) and blood (B), percentage of apoptotic cells (C), percentage of cells with associated bacteria (D) and percentage of neutrophils (E) in bronchoalveolar lavage (BAL) were calculated by analysis of cytopspins. n = 8 per group, *** = $p < 0.05$, students t-test.

10

1



2

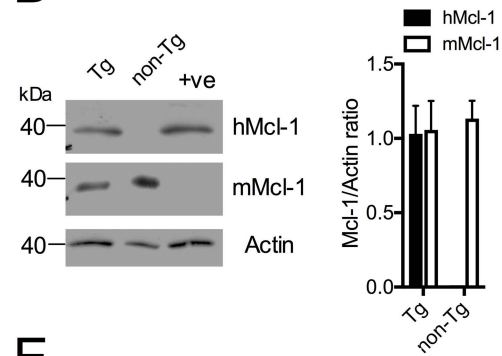
3 **Figure E11: *Staphylococcus aureus* infection does not trigger apoptosis-associated**
 4 **killing.**

5 (A) Bone marrow-derived macrophages (BMDM) from wild-type (non-Tg) or
 6 CD68.hMcl-1 transgenic (Tg) were mock-infected (MI) or challenged with *S. aureus*
 7 (Sa) at a MOI of 5. Cells were lysed at the designated time and probed for murine (m)
 8 Mcl-1. Blot representative of 3 independent experiments and cumulative densitometry
 9 presented. (B-C) Non-Tg or Tg BMDM were mock-infected (MI) or challenged with
 10 *S. aureus* at a multiplicity of infection (MOI) of 5, in the presence (+) or absence (-)
 11 of ABT737. 20 h post-challenge cells were assessed for nuclear fragmentation by
 12 microscopy (B) and, intracellular colony forming units (CFU) (C). In both
 13 experiments, n=3 and no significant differences were noted between groups or over
 14 time.

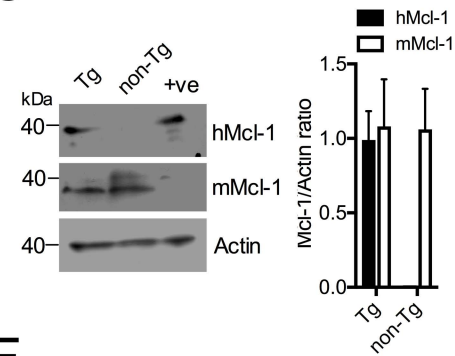
A CD68 5' flanking sequence IVS-1 Human Mcl-1 cDNA



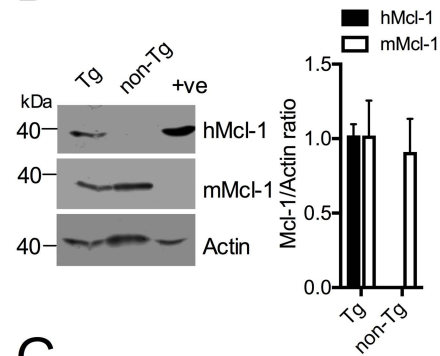
B



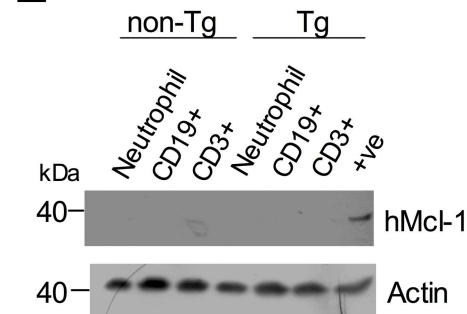
C



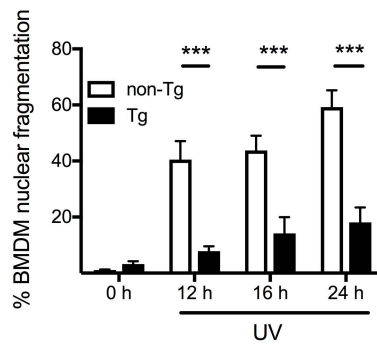
D



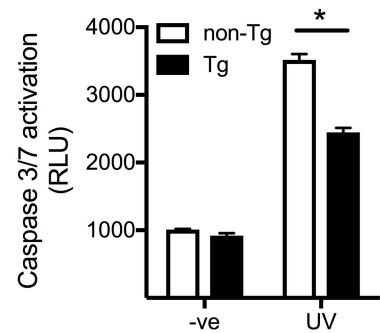
E



F



G



H

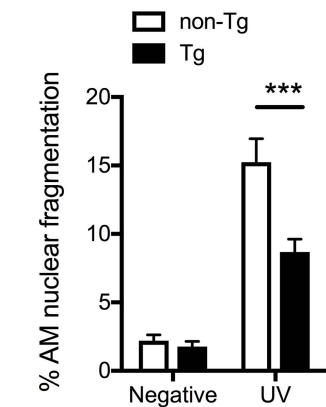


Figure 1

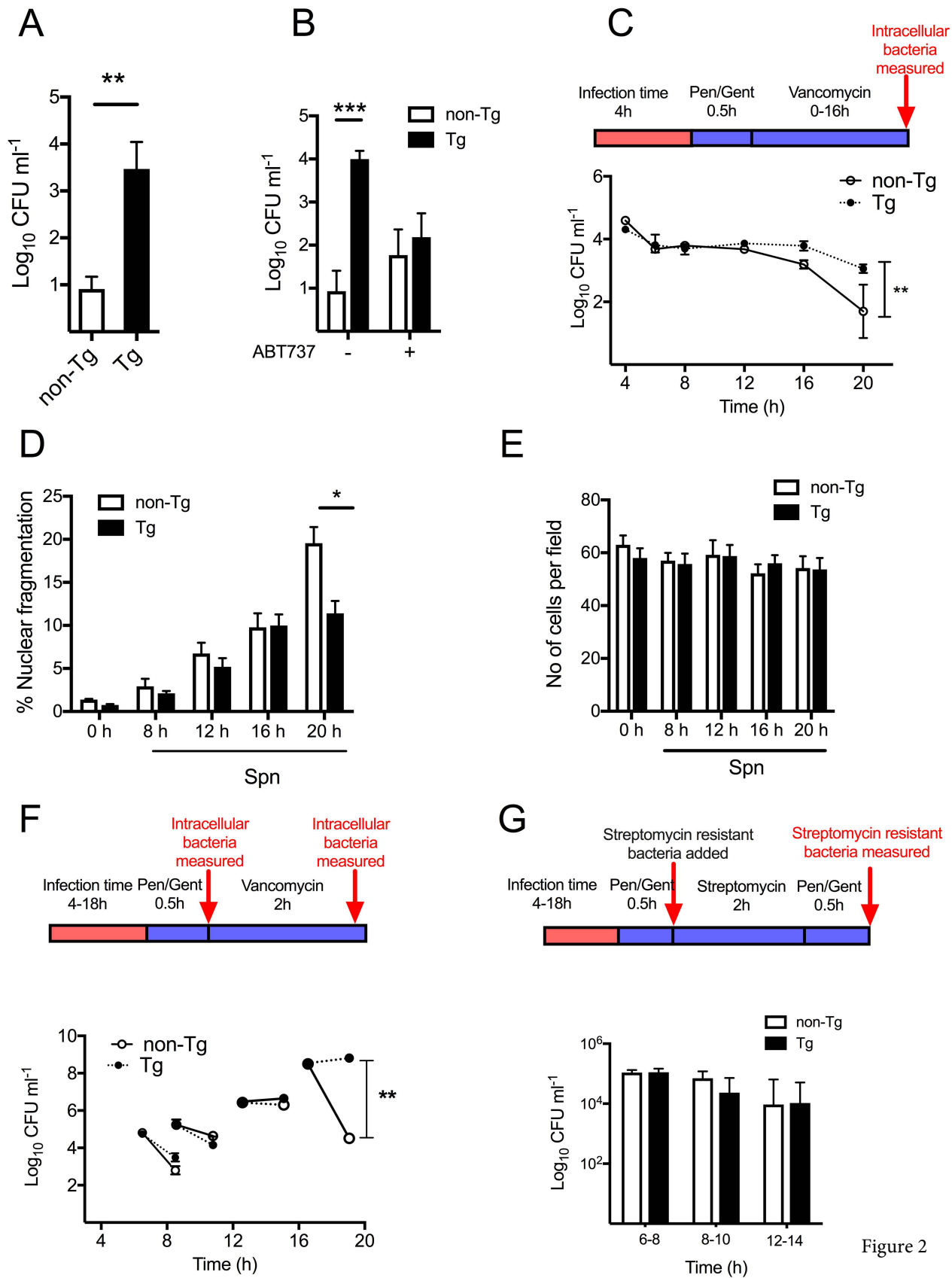


Figure 2

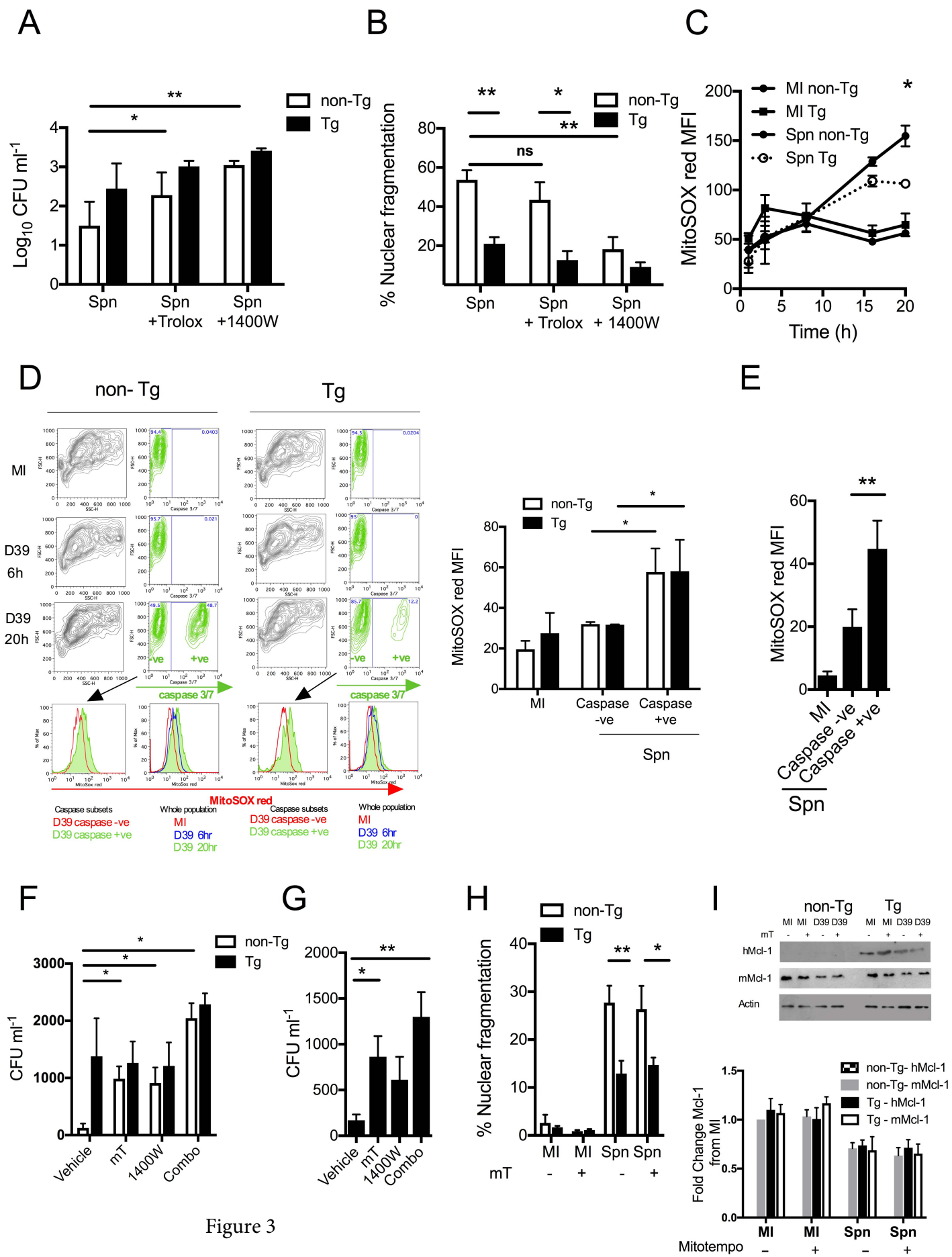


Figure 3

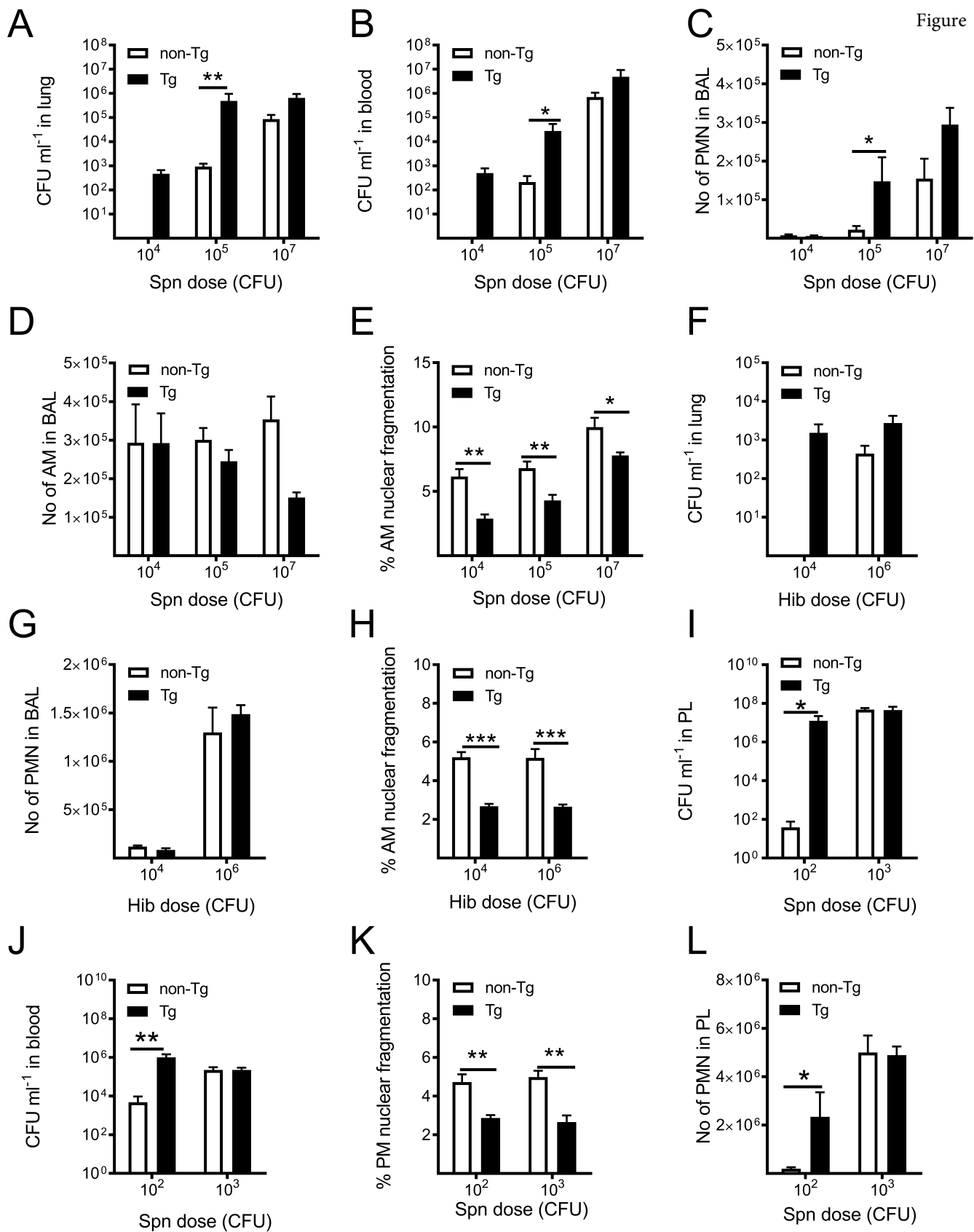
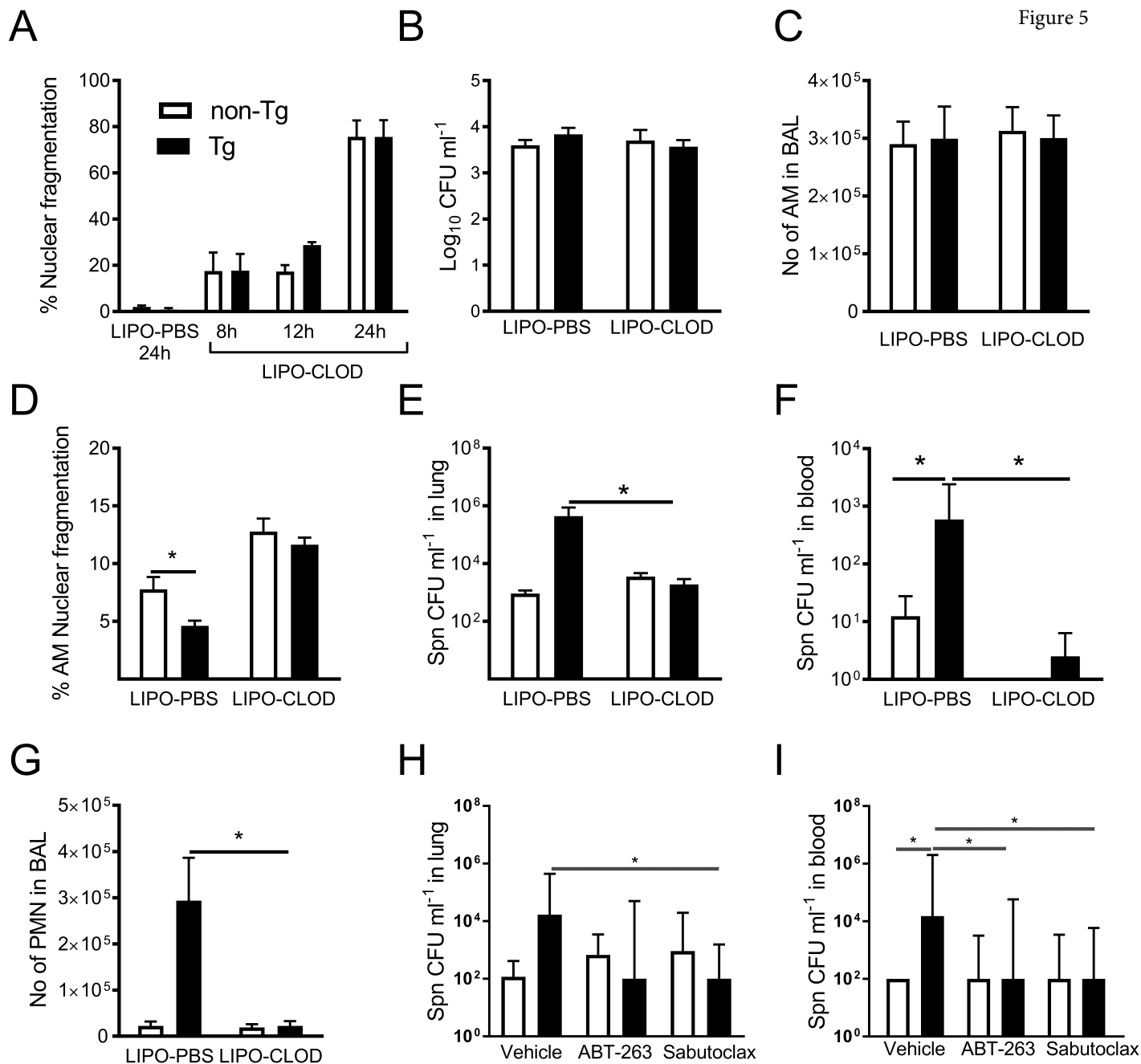


Figure 5



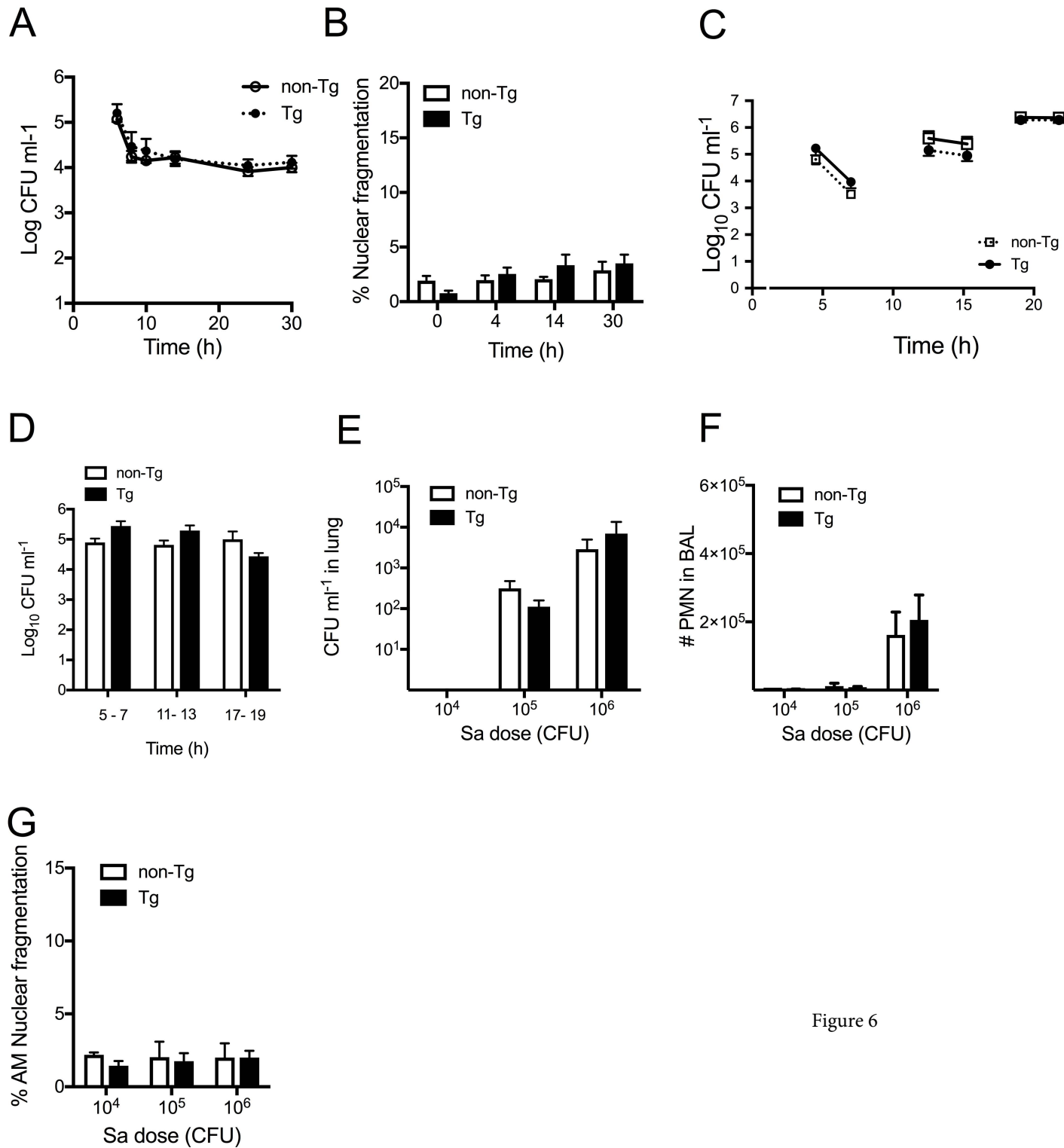


Figure 6